VIBRATION EXPOSURE FROM BUCKING BARS DURING PERCUSSIVE RIVETING IN THE AEROSPACE INDUSTRY

Wadih Zaklit

A thesis

submitted in partial fulfillment of the

requirements for the degree of

Master of Science in Mechanical Engineering

University of Washington

2018

Committee:

Per Reinhall

Joseph Garbini

Peter Johnson

Riley HansonSmith

Program authorized to Offer Degree:

Mechanical Engineering

University of Washington

Abstract

Vibration Exposure from Bucking Bars During Percussive Riveting in the Aerospace Industry

Wadih Zaklit

Chair of the Supervisory Committee:

Per Reinhall

Department of Mechanical Engineering

A study was done on several bucking bars used during percussive riveting. First a Simulink model was developed in order to predict a bucking bar's behavior depending on its mass, spring rate, and damping coefficient. The model was able to predict the actual testing with a RMSD = 7.74%. Then 5 different bucking bar handles were tested on an automated test bench and then Boeing mechanics used them to form rivets. The handles are 1 fixed plastic handle (P), 3 spring dampened handles (CS, CA, Y), and 1 spring and Sorbothane (T) handle. The results showed that the recoilless bars reduced the vibration by an average of 57.75% on the test bench compared to the fixed handle. The spring dampened bars showed a mean vibration reduction of 45% for mechanic 1 and of 16% for mechanic 2. There was no advantage of adding a damping material to a spring dampened bar.

List of Contents

List of Figures

List of Tables

Acknowledgements

- Professor Per Reinhall – Department of Mechanical Engineering, University of Washington, Seattle
- Professor Peter Johnson – Department of Environmental and Occupational Health Sciences, University of Washington, Seattle
- Riley HansonSmith – The Boeing company
- Kevin Oshiro – MathWorks
- Ryan Mott, Bryan Ford, Luke Wavrin, Szymon Sarnowicz, Cassidy Quigley, Livia Anderson, Frank Ryou – University of Washington, Seattle

Chapter I - Introduction

Aircraft production is an ever-growing industry and airplane manufacturers are always looking to raise their production rates. Manufacturing more airplanes doesn't come without a cost since each airplane requires intensive automated work in addition to manual labor. In order to build an airplane, its several metal sheet components have to be assembled together by using many hand held tools including rivet guns, sanders, grinders, and pneumatic wrenches. Some of these tools produce vibration that is transmitted to the mechanic which leads to long term traumas to their hands, shoulders, or back. Repeating the job every day, exposes the workers to higher risks of injury, therefore, proper and ergonomic tools are essential to protect the technicians and limit their exposure to high vibrations and forces.

Riveting is the most common method used to fasten or join aluminum alloys. It was first introduced in the 19th century when all rivets were still forged by hand. In aircraft construction and repair, riveting is an essential task. To build a Boeing 747, 6-million parts are needed, from which, 1.5-million parts are rivets. Each rivet is different in size and shape. For example, wing assembly requires larger rivets, so each rivet installation takes up to four seconds, while fuselage riveting requires smaller rivets, so it only takes about half a second to install a well-formed rivet.

Even though robots are used more often in manufacturing, a large portion of rivets are still installed manually. Two operators are needed to complete the job, one mechanic to operate the rivet gun which strikes the rivet's head and the other to hold

the bucking bar against the rivet's tail. In each factory, several rivet gun types and bucking bar designs are available and used depending on the application.

The bucking bar is usually made of an alloy steel similar to tool steel. Each bucking bar is unique as it has its own shape, weight, and diameter depending on the type of rivets being installed, but almost all bucking bars lack any sort of vibration dampening. Some modifications have been attempted in order to make the bucking bar more ergonomic and safer to use and the most popular adaptation is to use tungsten instead of steel. Tungsten is about 2.4 times denser than steel and has a bigger mass, resulting in less vibration emission to the human body [1].

A study done at the Boeing Advanced Research Center (BARC) compared a tungsten bucking bar to a steel bucking bar of the same size and shape and to a steel bucking bar of the same mass. It was concluded that the tungsten bucking bar dampened the vibration by 38% compared to the same size steel bucking bar and showed almost no improvement when compared to the same mass steel bar [2]. A similar study was conducted by Jorgensen and Viswantahan where they investigated tungsten and steel bars of the same size and shape for vibration during a riveting task. It was found that the tungsten bucking bars dampened the vibration by about 36% compared to steel bars [1].

Not all companies can afford switching from conventional steel bucking bars to tungsten bucking bars as they are much more expensive and more difficult to machine. There are other designs and interventions that focus on keeping a low cost while serving as vibration dampening. These interventions include rubber handles and spring-

loaded bucking bars. Yet few studies have examined those interventions in depth and tried to come up with better designs.

This study is split into three parts. The first part includes a model of the bucking bar system simulated via Simulink. It is intended to be used for future testing of different bucking bar designs. The second part focuses on building a new bucking bar handle that is aimed to reduce the vibration impact on the mechanic. Finally, the last part covers the testing of the new handle design versus other handles used across Boeing's factory floor. This thesis paper aims to measure the vibration level at the tool, the hand, wrist, forearm, and upper arm of the operator.

The sections of this study include a literature review which investigates the history and the research done in this field. Then a methods and theory section covers the theoretical background of all calculations with an explanation of the test plan. Finally, the results are presented with a detailed discussion and recommendations based on the objective and subjective data gathered during testing.

Chapter II - Literature Review

The amount of people employed in the United States is about 40% which means that a total of 130 million persons have a job. Out of those workers, 12.4 million work in manufacturing, according to U.S. Bureau of Labor Statistics. While only about 10% of the overall workforce is in manufacturing, workers in the latter field experience the most work-related injurie: 12.7% of the overall work-related injuries. The laborers who sustained occupational injuries and illnesses resulting in days away from work in 2015 required a median of 9 days to return to work [3].

Employees in the manufacturing field, especially in the aerospace industry are exposed to high levels of vibration, contact stress, and repetition. Riveters have to use vibration tools which negatively affect their hands, fingers, and overall body. They may also have eyes injuries caused by flying metals or long-term traumas resulting from the physical hard work that they have to endure. Some mechanics suffer from shoulder pain, musculoskeletal problems, and develop Raynaud's syndrome or vibration white finger.

The following section explains how vibration in the workplace can affect the human body. The format used is the same format used by the ISO 5349-1 to explain different disorders resulting from vibration exposure.

2.1 Vibration in the workplace

Vibration, periodic back-and-forth motion of the particles of an elastic body or medium, commonly result when almost any physical system is displaced from its equilibrium condition and is allowed to respond to the forces that tend to restore

equilibrium. Vibration is defined by its magnitude and frequency and is measured in three axes.

A vibrating system contains mass, elasticity, and damping components which enable the energy in the system to alternate between kinetic and potential energy. Without any mechanism to remove the energy from the system, the system would vibrate forever.

Vibration can cause changes in tendons, muscles, bones and joints, and can affect the nervous system. Whole Body Vibration (WBV) can be caused by poorly designed or poorly maintained vehicles, platforms, or machinery. Hand Arm Vibration (HAV) can be caused by long term exposure from using hand held tools such as pneumatic tools, chainsaws, grinders etc. Employees whose hands are regularly exposed to vibration may suffer from damage to the tissues of the hands and arms [4]. These conditions can have negative effects on people and they can be permanently disabling even after a few years of uncontrolled exposure [5].

2.2 Hand Arm Vibration

Hand-Arm Vibration Syndrome (HAVS) is the medical term for symptoms caused by vibration damages that may occur in the fingers, hands, and arms when working with vibrating tools or machinery [6]. Muscular weakness, decreased grip strength and pain in the wrists, elbows, neck, and back may occur among vibration-exposed workers [7]. HAVS is a painful and potentially disabling condition that may lead to a reduction in the quality of life.

Its effects can be divided into neurological, vascular, and musculoskeletal disorders. Workers in percussive riveting experience more neurological and musculoskeletal disorders than vascular. The high-frequency region vibration may be responsible for damage to the soft structures of the fingers and hands, while low-frequency vibration of high amplitude (percussive tools) might be associated with injuries to the wrist, elbow, and shoulder [8].

2.3 Neurological disorders

Burdorf and Monster investigated riveters and controls in an aircraft company for the effect of vibration exposure and health complaints [9]. They studied 101 riveters and 76 controls with no, or little exposure to vibration. The results of the cross-sectional study provided some evidence that the use of impact power tools and exposure to vibration could result in pain and stiffness in the hand, arm and shoulder, and especially in the wrist.

Azmir et al. studied the effect of hand arm vibration on the development of vibration induced disorders among grass cutter workers [10]. They chose 204 hand held grass cutter workers to participate in the experiment for 5 months. Their study concluded that more than 90% of the workers developed an at risk stage of compromised hand grip strength. They also added that about 80% had a vascular disorder above stage 2 in both of their hands.

Nilsson et al. conducted a systematic review and meta-analysis of the literature on the association of neurological diseases to hand-arm vibration [11]. They covered

the scientific literature up to January 2016 and concluded that workers who are exposed to HAV are 4 to 5 times more likely to develop a vascular and neurological disease.

2.4 Musculoskeletal disorders

According to the US Bureau of Labor Statistics, musculoskeletal disorders (MSDs) accounted for 32% of all nonfatal injury and illness cases in 2014 among full-time workers. From 1999 to 2004, manufacturing was one of the industries with the largest number of claims (25.1%). Charles et al. conducted a study to relate occupational exposures to vibration and awkward posture with MSDs of the shoulder and neck [12]. It was concluded that occupational exposures to whole-body or hand–arm vibration were significantly associated with or resulted in MSDs of the shoulder and neck.

Bonvenzi et al. published a study investigating the bone and joint disorders in the upper extremities of chipping and grinding operators [13]. The study showed that muscle pain and decreased muscular force significantly increased in the chipping and grinding workers compared to workers performing heavy manual work. They added that the overall prevalence of radiographic abnormalities in the elbow joint was higher in the vibration group than the control group.

Bovenzi continued his research and studied 64 vibration-exposed operators using chain-saws to 31 comparable subjects performing manual activity and not exposed to vibration [14]. Bovenzi and his team observed significantly higher prevalence rates of persistent upper limb pain and muscle-tendon syndromes among the forestry workers and not among the controls. They also noted that in the forestry

operators, the occurrence of upper limb musculoskeletal disorders increased with increasing vibration exposure.

Characteristics of percussive tools such as vibration frequencies around 30 Hz and the high magnitude or amplitude of shocks may be the main cause of bone and joint disorders [15]. Kihlberg and Hagberg studied hand and arm symptoms such as pain, numbness, and finger blanching among workers using impact and non-impact hand-held power tools [16]. Workers using low frequency impact tools reported more symptoms in the elbows and shoulders. Wrist symptoms were reported more frequently by those working with the high frequency impact tools.

Hagberg performed a clinical assessment of musculoskeletal disorders in workers exposed to hand-arm vibration [17]. Hagberg's experiments showed that low-frequency vibration exposure of high magnitude was associated with osteoarthritis in the elbow and wrist. He also added that the scientific evidence that vibration per se is a risk factor for musculoskeletal disorders is still weak although there is strong evidence that job tasks with vibrating machines are associated with musculoskeletal disorders.

2.5 Vascular disorders

The symptoms were first described by Professor Giovanni Loriga in Italy in 1911, but it wasn't before 1918 that Alice Hamilton MD was able to make a connection between the symptoms and vibrating hand tools. In 1970, the Industrial Injury Advisory Council named vibration-induced white finger (VWF) a disorder that affects the blood vessels, nerves, muscles, and joints, of the hand, wrist, and arm.

Dandanell and Engstrom explored the effects of vibration from riveting tools in the frequency range 6 Hz-10 MHz on the Raynaud's phenomenon [18]. In a group of 288 riveters, about 50% showed symptoms indicating Raynaud's phenomenon (VWF) after about 10 years of work, although the daily exposure of riveting tools was about 1 min/day.

Early stages of vibration syndrome are characterized by tingling or numbness in the fingers [19]. The symptoms usually appear suddenly and cold is a big factor in making the symptoms worse. With continuing exposure to vibration, the signs and symptoms become more severe and the pathology may become irreversible [19]. The severity of vibration syndrome can be measured using a grading system developed by Taylor where stage 00 is no tingling, numbness, or blanching of fingers and stage 04 is extensive blanching of most fingers; during summer and winter [20].

To be diagnosed as vibration syndrome, the neurologic symptoms must be more persistent and occur without provocation by immediate exposure to vibration. After a clinical observation and an interview, a worker can be placed into one of the categories found in Table *1*, developed by Taylor and Pelmear.

Table 1: Stages of Raynaud's Phenomenon (Taylor and Pelmear, 1975)

Stage	Condition of fingers	Work and social interference
00	No tingling, numbness, or blanching of fingers	No complaints
OT	Intermittent tingling	No interference with activities
ON	Intermittent numbness	No interference with activities
TN	Intermittent tingling and numbness	No interference with activities
01	Blanching of a fingertip with or without tingling and/or numbness	No interference with activities
02	Blanching of one or more fingers beyond tips, usually during winter	Possible interference with nonwork activities; no interference at work
03	Extensive blanching of fingers; during summer and winter	Definite interference at work, at home, and with social activities; restriction of hobbies
04	Extensive blanching of most fingers; during summer and winter	Occupation usually changed because of severity of signs and symptoms

A number of factors influence the development of VWF and the most important ones are the frequency, amplitude, and direction of vibration, the contact between the tool and the subject, and the overall vibration exposure. The International Organization for Standardization (ISO) summarized that the severity of the biological effects of hand-transmitted vibration is influenced by the frequency spectrum of vibration, magnitude, and direction of forces, by the tool's type, and by the location of the parts of the hand

being exposed. The duration of exposure per working day, the temporal exposure pattern, and the cumulative exposure to date also impact the severity of biological effects (ISO 5349, 1986).

2.6 Standards for vibration exposure

Vibration measurement is a description of motion expressed in terms of both magnitude and direction. The magnitude of hand-arm vibration is quantified as the acceleration rate in an engineering unit known as "meters per second squared" (m/s^2). The exposure action value (EAV) is a daily amount of vibration exposure above which employers are required to action to control exposure. The greater the exposure level, the greater the risk and the more action employers will need to take to reduce the risk. For hand-arm vibration the EAV is a daily exposure of 2.5 m/s^2 and the exposure limit value (ELV) is 5 m/s^2 and it represents a high risk above which employees should not be exposed.

HAV exposures are of concern when the vibration occurs within a certain frequency range. This range is identified by ISO 5349 as nominally 5.6 Hz to 1,400 Hz. The ISO 5349 standard was developed in 1986 and then updated in 2001. The standard is used to define acceptable exposure limits. However, this standard is better suited for steady state vibrating tools rather than low frequency vibration impact tools [19].

Troell et al. conducted a study to address the society challenge to reduce vibration injuries, today the most common cause of occupational disease in Sweden [21]. They noted that the high frequency content of vibrations, above 1250 Hz that ISO 5349 does not include, has to be included since it is a potential risk for causing

substantial vibration injuries. They concluded by saying that a new standard or supplementary standard to ISO 5349 is needed to cover all the frequency ranges.

In the 7th American Conference on Human Vibration, Lundström, in his paper about Vibration Produced by Percussive Hand Tools Is an Underestimated Contributor to The Development of Vibration Injury [22], and Lindell in his study of High Frequency Vibration and its effects on biologic tissue [23], both suggested a revision of ISO 5349, or at least an amendment or appendix to it to cover high frequency and/or percussive vibration. They also added that there are several studies that show that ISO 5349 underestimates the risk for injuries from high frequency transient vibrations.

2.7 Bucking bar modifications - Handles and Material

Boileau studied the hand arm vibration associated with the use of riveting hammers in the aerospace industry and noticed that the bucking bar operator is exposed to vibration level which can be 3-5 times the levels recorded for the riveting hammer operator [24].

Several studies have investigated how bucking bar interventions could reduce the vibration emission to the operator. Some researchers addressed the issue by changing the material of the bucking bar and they focused on tungsten and steel, some others looked into the handles of the bars and how can they make them more ergonomic.

In 2017, a team of students, faculty, and Boeing engineers performed a study investigating the material and mass of the bucking bar and their effects on vibration emission [2]. It was concluded that tungsten and steel of the same mass performed

equivalently under the ISO 5349-1 standard. They also added that tungsten showed almost 50% reduction in vibration compared to a same geometry steel bucking bar.

Jorgensen and Viswanathan looked into the ergonomic field assessment of bucking bars during the riveting process [1]. Four different bucking bars of the same shape but different material and mass characteristics (90% tungsten, >90% tungsten, cold rolled and stainless steel) were investigated for vibration and grip muscle activity during a riveting task. The results suggested that for bucking tasks that allow access for the bucking bar size investigated, use of heavier but same sized tungsten bucking bars can reduce vibration transmission to the hand.

McDowell assessed rivet bucking bar vibration emissions [25]. The study evaluated three traditional steel bucking bars, three similarly shaped tungsten alloy bars, and three bars featuring spring-dampeners. For comparison, the bucking bar vibrations were also assessed during three typical riveting tasks at a large aircraft maintenance facility. Tungsten bars and similarly sized bucking bars incorporating spring-dampeners exhibited significantly reduced vibrations compared to the traditional steel bars.

Adding a handle to a tool is one way to modify the amount and the location of vibration transmitted into the body [26]. Cherng et al. attempted ergonomic re-design approaches on both the rivet gun and bucking bar [27]. Rivet tools with vibration damping/isolation mechanisms were tested against two conventional rivet tools in both laboratory and field tests. The overall conclusion obtained from the study was that by applying the design principles of ergonomics and by adding vibration damping/isolation

mechanisms to the rivet tools, the vibration level can significantly be reduced, and the tools become safer and more user friendly.

Hull studied the Perceived Usability of Ergonomic Interventions for Steel Bucking Bars [28]. The interventions included a tungsten bucking bar, Viscolas® rubber wrap adhered to a steel bucking bar, a steel bar paired with an anti-vibration glove, and a steel bar with a detachable handle. The tungsten bucking bar was determined most usable in terms of perceived exertion and willingness to recommend to others while he steel bucking bar was not favored by any of the participants as they ranked the steel bucking bar the lowest.

Chapter III – Methods and Theory

To analyze the data acquired during testing, the analysis was split into 2 parts: a quantitative and a qualitative approach. The quantitative approach takes into consideration the measurements and data collected from all the sensors mounted on the tools and operators. It analyzes the data mathematically and objectively. The qualitative approach takes into consideration the operators' feedback and their rating of each tool based on their own experience using it.

3.1 Quantitative

1. Tools

The rivet gun, shown in *Figure 1*, was used and is an Atlas Copco RRH 10P-TS (AC-10P) with a serial number A6710012 and mass of 2 kg. This rivet gun is a recoilless rivet gun designed to absorb impacts and reduce the potentially harmful effects to the operator. It includes vibration damping, as well as adaptable power, so it can be used to form a variety of rivet types and sizes. This rivet gun is typically used in the Boeing, Everett factory for fuselage rivets.

Figure 1: AC-10P rivet gun used during testing. It is the standard recoilless gun used at Boeing for fuselage riveting.

The bucking bar, pictured in *Figure 2*, was used for the testing. It is custom made to match the size and mass of typical bucking bars used for fuselage riveting. It's made out of 4140 steel (per material callout in Boeing ST30-1000-CN Rev AB drawing). The bucking bar's total length is 7" with a square 2"x2" surface area and a mass of 2.8 kg.

Figure 2: Steel bucking bar used during testing. It has typical bucking bar mass for fuselage riveting.

The rivets, shown in *Figure 3*, are the same rivets used on airplane fuselage and are made of Aluminum alloy 7050-T73. Their dimensions are summarized in Table *2*.

Figure 3: Rivet used during testing. It is the standard rivet used on an airplane's fuselage.

Table 2: Summary of the rivet's dimensions.

Diameter, D (in)	0.221
Total length, L (in)	0.442
Length except countersunk head, Lh (in)	0.38
Angle of countersunk head of rivet, α (°)	120

In order to replicate the fuselage, a rectangular aluminum sheet called a coupon was used. It is a single ply sheet made out of 2324-T39 aluminum, the same aluminum type of an airplane's fuselage, and was cut to the size 6"x15"x0.19". It was fixed on the test bench along all of its edges. 12 identical holes of 7/32" diameter with a 120° countersink and 5/16" counter bore diameter were drilled in the coupon, as seen in Figure *4*.

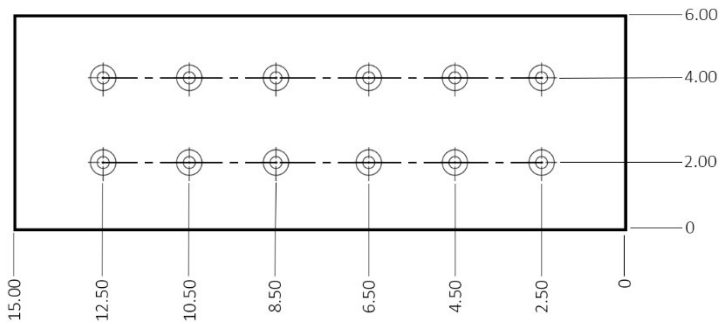

Figure 4: Hole pattern of all coupons used during testing. A total of 12 equally spaced holes were drilled into a 0.19" thick Aluminum sheet.

Five different handles were tested with the same bucking bar. A Plastic Handle (P), shown in *Figure 5*, is the standard plastic handle used throughout the Boeing

manufacturing floor; it was used as the baseline for this study. A Spring Handle (Y), illustrated in *Figure 6*, made out of steel with an interior spring (spring rate of 26.5 lbf/in) to minimize vibration emission and absorb energy, is used during testing. Boeing mechanics were experiencing a few problems with the Y handle: some mechanics reported the bolt breaking and the bar shooting out of its handle, or that the bar is hard to control. Therefore, two modified spring handles, CS and CA, shown in *Figure 7*, and *Figure 8* were based of the Y handle and were developed in the BARC Lab to address those problems. The CS and CA still use a handle with an interior spring (spring rate of 26.5 lbf/in) to minimize vibration emission and absorb energy, but they are made from steel and aluminum respectively with an updated handle cover (polymer 50 durometer), bolt, holes, and overall length. Finally, a spring and Sorbothane handle (T), pictured in *Figure 9* was put to test. It is a steel handle covered in Sorbothane with an interior spring (spring rate of 34 lbf/in). The polymer inside is a 1” thick and 1.38” diameter cylinder made of a 70 durometer (based on shore “00” scale) polymer. The handle cover should have been 0.15” thick along the edges and 0.42” thick at the bottom and made out of 30 durometer (based on shore “00” scale) polymer. Due to time constraints, another polymer with a higher durometer was used instead.

Figure 5: Plastic handle (P) used during testing.

Figure 6: Spring Handle (Y) used during testing.

Figure 7: Modified Steel Spring Handle (CS) used during testing.

Figure 8: Modified Aluminum Spring Handle (CA) handle used during testing.

Figure 9: Spring and Polymer handle (T) used during testing

2. Instruments

Using a National Instrument's PXI machine running LabVIEW, the data was collected using various sensors during automated testing and manual testing. Once the data was successfully recorded, it was analyzed using Microsoft Excel and Matlab. The sensors used to acquire the data are as follows:

- Shock accelerometer: The accelerometer used is fixed to the bucking bar. It is a PCB 350C04 shock accelerometer with a serial number 58868. This sensor is rated to measure within an amplitude range of -5,000 to 5,000 g's amplitude at 1.0mV/g

and within a frequency range of 0.2 to 25,000 Hz. This sensor recorded axial accelerations of the bucking bar itself at 20,000 Hz.

- Tri-axial accelerometer: The tri-axial accelerometer is a Larson Davis SEN040F with a serial number P109499. It is rated to measure within an amplitude range of -5,000 to 5,000 g's within a frequency range of 2 to 4,000 Hz in the X, Y and Z directions. This accelerometer was used to collect acceleration data from the handle of the bucking bar at 20,000 Hz.

- Load cells: The load cells were used on both the rivet and bar side for both automatic and manual tests are Interface WMC-500 mini load cells. They are rated to measure within a range of -500 to 500 lb. Their serial numbers are 601431A and 601447A. These sensors are used to measure the push force as well as the recoil force of the bucking bar and rivet gun. They were sampled at 10,000 Hz.

- Laser displacement sensors: The laser is used on the bar side for automated testing. The laser is made by Keyence, its model is LK-H152 displacement sensors. This sensor is used to measure the displacement of the bar at 10,000 Hz.

- ICP Force Sensor: The force sensor is a PCB 200B50 load cell. It is rated to measure within a range of -50,000 to 50,000 lbf. The load cell was mounted on the bucking bar on the test bench and was used to form a few rivets in order to collect force data at 200,000 Hz.

- Flow Rate: To record flow rate, two pressure transducers (Serials: 2X394813 and 2X370139) and a temperature transducer from within the Boeing Company were used in conjunction with custom venture designed by Flowmaxx Engineering PN

VF16-SA-285. This information was used to verify the correct operation of all tools and to ensure that air pressure was consistent and did not act as a free variable.

- Inertial Measurement Unit (IMU): This device measures acceleration using a MEMS-based triaxial accelerometer. A total of 6 IMUs were used during manual testing and were strapped on each mechanic. The location of the IMUs were on the hand, forearm, and arm on each side of the mechanics' bodies. They were used to collect acceleration data at each given location and to study the vibration transmissibility in the hand-arm system. They were sampled at 3,200 Hz.
- HavWear: The HavWear sensors (made by REACTEC) are wrist mounted and used during manual testing. The sensors are designed to monitor vibration exposure on the wrist. Raw data is processed through the product's transfer function which is based on the 5349-1 standard.

3.2 Qualitative

After each round of testing and when the mechanics were done installing all the rivets using a handle and bucking bar, they were asked to fill out a survey. The questionnaire was based on a 1-7 scale where 1 is strongly disagree and 7 is strongly agree. The questions asked were:

1. This tool was easy to use
2. This tool feels comfortable to my hands and wrists while using
3. This tool feels comfortable to my arms and shoulders while using
4. It was easy to make errors using this tool

5. I liked the weight of this tool
6. I can quickly complete tasks using this tool
7. I like the overall feel of this tool while using
8. There were less vibrations when using this tool
9. It took a long time to adjust to this tool
10. I like the handle of this tool

3.3 Testing Procedure

Testing was split up into 2 parts: automated and manual testing. Automated testing used the test bench developed and built in BARC. The test bench controlled factors such as position of the gun and the bar, trigger pull rate, and push force. For the manual testing, 2 Boeing experienced mechanics were brought to the lab and formed rivets. During testing, each of the handles is used 3 times (test bench and 2 mechanics) to form 12 rivets every time.

3.3a Automated testing

Automated testing was conducted using the automated test bench located in the BARC on the University of Washington campus in Seattle. The test bench is pictured below in *Figure 10*.

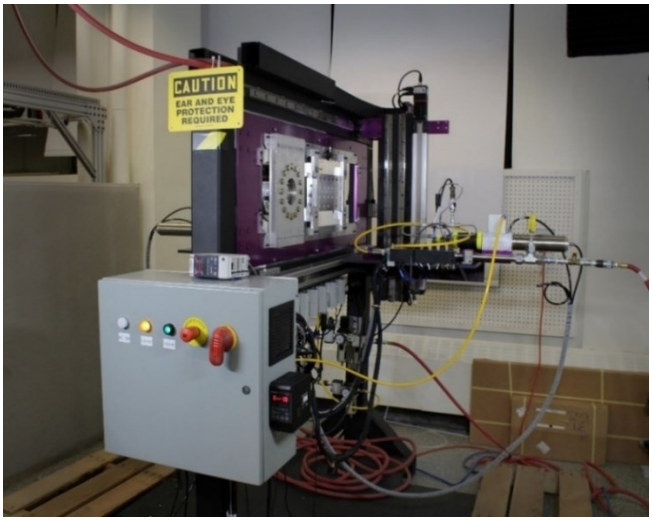

Figure 10: Automated test bench developed in the BARC at the University of Washington, Seattle

The rivet gun was secured to the test bench by a 3D printed ABS plastic collar attached to a nearly frictionless linear roller equipped with rail ball bearings. Smaller plastic collars were inserted into the original piece to allow it to be used for tools of different diameters. To reduce the number of independent variables, the same die and die retention spring were used for all tests. These constants are pictured in *Figure 11*.

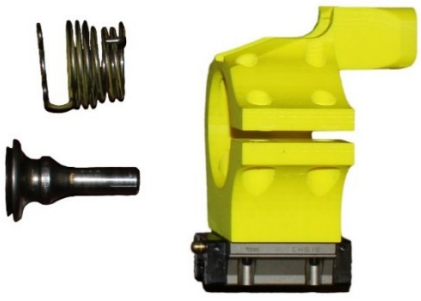

Figure 11: Hardware used during automated testing. Retention spring is on the left upper corner, the die is on left bottom corner, and the collar is on the right.

The trigger of the gun was activated by a pneumatic cylinder propelling a metal rod to fully compress the trigger. This allowed to control the cycle time of each rivet which was fixed at 0.5 second. This cycle time allowed the rivets' diameter to be within specifications (0.33"-0.4").

The gun supplied a push force similar to what is expected from a mechanic using the same tools and the same size rivets. The supplied push force was 55 lbf and was exerted for 0.5 second by the help of an air cylinder attached to the test bench. The load cell described above was threaded into the air cylinder and connected to the rear of the gun, which is suspended by the collar described above.

The bucking bar side of the test bench used a similar setup. A steel mass designed to mimic the mass of the human arm was mounted behind the bucking bar. The force supplied was transferred through a synthetic "forearm" made of a Delrin rod with a spring constant similar to that of a human forearm. An air cylinder provided a push force to the rear of the bar and a load cell was mounted as on the rivet gun side. The supplied push force is similar to what is expected from a mechanic and was 30 lbf.

3.3b Manual testing

For manual testing, two experienced Boeing mechanics installed rivets on the test bench for comparison. The gun side was automated to provide consistent forces and rivet time. The test bench environment attempts to mimic actual field-based riveting and bucking installations. This manual testing gives insight into how well the test bench replicates the riveting process. After every session, the rivet diameter was measured and recorded to ensure that the mechanics and the test bench formed consistent rivets.

3.4 Simulink model

In order to be able to model the bucking bar, it is assumed that it acts like a mass-spring-damper fixed at one end. The parameters of the system needed to be identified for them to be used in the Simulink model. Some experiments involving a step input, an impulse input, and a hysteresis test were done to find the spring constant, damping in the system, and friction.

Bucking Bar System

For all experiments, the steel bucking bar was fixed in a vertical position and the bolt was removed so the bucking bar was free to move without hitting its hard stops. Its displacement was recorded using a laser displacement sensor and its acceleration was measured by a shock accelerometer. The setup can be seen in *Figure 12* below.

Figure 12: Bucking bar system setup for Simulink experiments.

1. Spring rate

To calculate the spring rate, the bucking bar was installed on an Instron machine which recorded the load being exerted and the displacement of the bucking bar. Using Hook's law summarized in equation 1, the spring rate was calculated.

$$F_s = K * x \tag{1}$$

Where F_s is the force being exerted, K is the spring rate, and x is the displacement of the bucking bar.

2. Hysteresis

The bucking bar was placed in an Instron machine that applied a cyclical load on it. Using the data collected and by studying the hysteresis loop, the system parameters were calculated and identified. Equation 5 shows how the friction was calculated.

$$\Delta w = 4 * F_c * X \tag{2}$$

Where Δw is the energy dissipated in 1 cycle, F_c the force of friction, and X the max deflection of the spring.

3. Step input

Using the tungsten bar as a step input, it was placed right above the steel bar and let go. The system oscillated and then came to a stop. Using the data from the laser and the equations of a mass spring damper system with a unit step input, the system parameters were calculated and identified. From the percent overshoot, seen in

equation 2, the damping ratio was calculated. And then using equation 3, the damping coefficient was found.

$$PO = e^{-\frac{\pi\zeta}{\sqrt{1-\zeta^2}}} * 100 = \frac{x_{peak}-x_{ss}}{x_{ss}} * 100 \quad (3)$$

$$c = 2 * m * \zeta * w_n \quad (4)$$

Where PO is the percent overshoot, ζ is the damping ratio, x_{peak} is peak displacement value, x_{ss} is the displacement value at steady state, m is the mass of the bucking bar, and w_n is the natural frequency of the system.

4. Impulse input

Using a hammer, the bar was hit once and left free to oscillate before coming to a stop. Using the data collected and the equations of a second order system with an impulse input, the system parameters were calculated and identified. Using equation 3 and the log decrement shown in equation 4, the damping ratio and coefficient was found.

$$\delta = \frac{1}{n} * \ln(\frac{x(t)}{x(t+nT)}) \quad (5)$$

Where δ is the logarithmic decrement, n is the number of successive positive peaks, $x(t)$ is the displacement amplitude at time t, $x(t+nT)$ is the displacement amplitude at n periods away.

The rivet gun

In order to be able to model the rivet gun, it was decided to isolate the rivet gun side and only focus on the bucking bar system. An ICP Force sensor was mounted on the bucking bar, as seen in *Figure 13*, and was used to form the rivets. With that configuration, the load cell would only be measuring the force coming out of the rivet and transferred to the bucking bar. Then, using the measured force data, a Fourier series approximation was done, and the estimated function was used as an input to the Simulink Model. *Figure 13* and *Figure 14* below show the setup of the bucking bar and load cell.

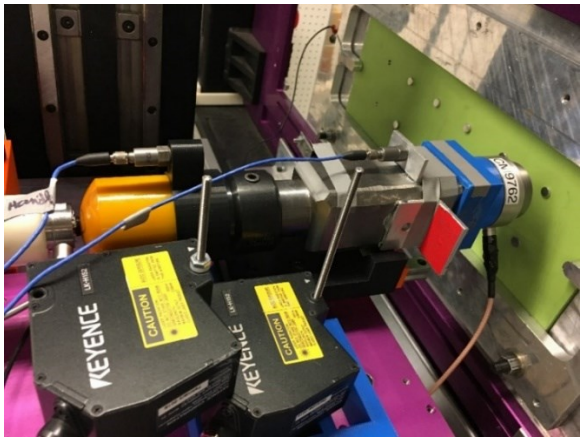

Figure 13: Bucking bar setup with a load cell attached to it and used to form the rivets. The load cell measured the force from the rivet to the bar.

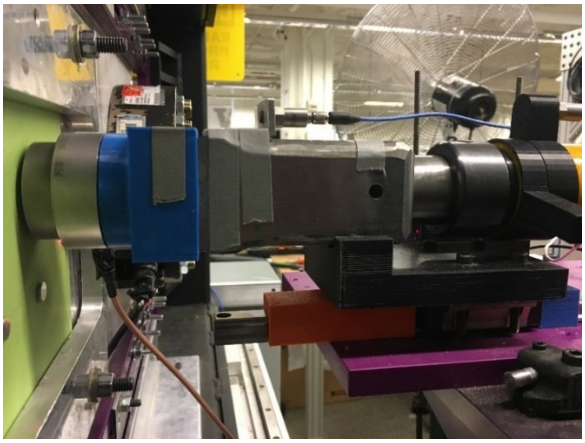

Figure 14: Close up of the load cell attached to the bucking bar and used to form a rivet.

The rivet

In order to able to model the rivet, it was critical to determine the rivet's dimensions and material. The material was determined to be AL 7050-T73. Using the

specific stress strain curve and the Ramberg-Osgood equation, the deformation was calculated after each hit.

$$\varepsilon = \frac{\sigma}{E} + K\left(\frac{\sigma}{E}\right)^{n} \quad (6)$$

Where ε is the strain, σ is the stress, E is the Young's Modulus, K and n are constants that depend on the material being considered.

It was assumed that the body of the rivet inside the coupon is not deforming and that the tail of the rivet was deforming as a cylinder with a constant volume. *Figure 15* details how the assumption was made. It was also assumed that the rivet had a constant stiffness and damping.

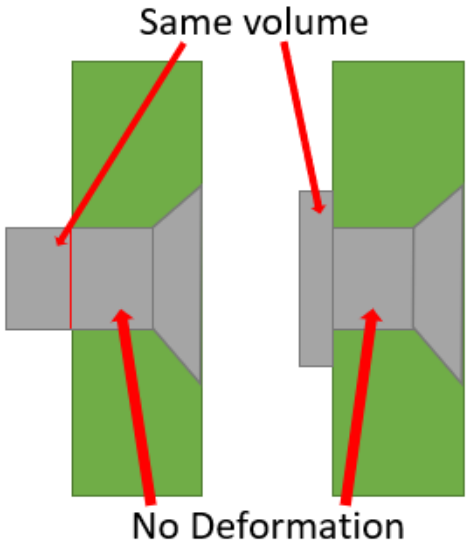

Figure 15: Rivet deformation schematic.

Root-mean-square deviation

The root-mean-square deviation (RMSD) is a frequently used measure of the differences between values (sample or population values) predicted by a model or an

estimator and the values observed. It is used to compare the actual recorded data to the simulated results on Matlab and Simulink. A calculated value less than 10% means that the model can accurately mimic the real-life experiment. The equation used to find the RMSD is:

$$RMSD = \sqrt{\frac{\sum_{t-1}^{T}(\widehat{y_t} - y_t)^2}{T}} \quad (7)$$

Where $\widehat{y_t}$ is the predicted value, y_t is the measured value, and T is the number of times the variable is predicted.

3.5 Bucking bar handle design

The design of the new bucking bar handle faced a few constraints. In order to be able to use the same bucking bar with the new handle, its inner diameter couldn't be changed. That limited the choice of spring that can be used. Also, the overall size of the handle is very important because sometimes the mechanics would have to rivet in tight spaces. Taking that into consideration, a new handle, with the goal of shock absorbing and vibration isolating, was developed.

Some mechanics reported that the spring handle was hard to control and that a stiffer spring should be used. The mechanics usually push with about 30 lbf on the bucking bar which limits how stiff the spring could be. The spring chosen had a spring rate of 34 lbf/in and the handle was designed so when the riveters push with 30 lbf, the dowel pin holding the bucking bar would sit in the middle of the notch which allows oscillation without hitting the hard stops.

A few other workers complained about the bolt holding the bucking bar in its handle was breaking. To solve the problem, a dowel pin with a higher shear strength was used instead. The holes on the handle were designed so that the dowel pin had a slip fit in 1 hole and press fit in the other.

3.6 Vibration Isolation

To isolate the vibration, a visco-elastic polymer was used. It is placed inside the handle to isolate the spring's oscillations. To determine the polymer's type, size, and thickness, equations 8 through 19 were used (Sorbothane Engineering design guide).

$$SF = \frac{D}{4t} \tag{8}$$

Where SF is the shape factor, D is the diameter of the polymer, and t its thickness. The shape factor determines how soft or hard the polymer is, and it should fall between 0.3 and 1.0.

$$CM = \frac{CS}{assumed\ \%\ deflection} \tag{9}$$

Where CM is the compressive modulus, CS is the compressive stress found from *Figure 52* in appendix A.

$$CM_{corr} = CM * (1 + SF^2) \tag{10}$$

Where CM_{corr} is the corrected compressive modulus.

$$Load = \sqrt{F_m^2 + m * K * v^2} \tag{11}$$

Where $Load$ is the load per isolator, m is the mass of the bucking bar, K the spring rate, v is the initial velocity of the bucking bar, and F_m is the push force of the mechanic.

$$\delta_{st} = \frac{load*t}{CCM*A} \tag{12}$$

Where δ_{st} is the static deflection and A the area of the isolator.

$$\%\delta = \frac{\delta_{st}}{t} * 100 \tag{13}$$

Where $\%\delta$ is the percent deflection and it should agree within 3% of the assumed percent deflection.

$$K_{dyn} = \frac{E_{dyn}(1+2*SF^2)*A}{t} \tag{14}$$

Where K_{dyn} is the dynamic spring rate and E_{dyn} is the compressive modulus found in *Figure 53* in appendix A.

$$f_n = \frac{\sqrt{\frac{K_{dyn}*g}{Load}}}{2*\pi} \tag{15}$$

Where f_n is the system's natural frequency and g is the acceleration of gravity. The calculated frequency should agree within 3% of the assumed natural frequency which was assumed to be $\frac{1}{3}$ of the forcing frequency.

$$r = \frac{f_e}{f_n} \tag{16}$$

Where r is the frequency ratio and f_e is the assumed natural frequency.

$$G_{dyn} = \frac{E_{dyn}@(f_n)}{E_{dyn}@(f_e)} \quad (17)$$

Where G_{dyn} is the dynamic shear ratio.

$$T = \sqrt{\frac{1+td^2}{(1-r^2 G_{dyn})^2+td^2}} \quad (18)$$

Where T is the transmissibility and td is found in *Figure 54* in appendix A.

$$\%I = (1 - T) * 100 \quad (19)$$

Where $\%I$ is the percent isolation.

3.7 Shock Isolation

To isolate the shocks, a visco-elastic polymer was used as a cover to the handle. To determine the polymer's type, size, and thickness, equations 20 through 23 were used (Sorbothane Engineering design guide).

$$\delta_{st} = 0.2 * t \quad (20)$$

Where δ_{st} is the static deflection and t the thickness of the isolator.

$$KE = \frac{1}{2} m v^2 \quad (21)$$

Where KE is the kinetic energy of the bucking bar.

$$K = \frac{W}{\delta_{st}} \quad (22)$$

Where K is the stiffness of the isolator and W is the weight for deflection.

$$\%\delta = \frac{\delta_{st}}{t} * 100 = \frac{\sqrt{\frac{2*KE}{K}}}{t}*100 \quad (23)$$

Where $\%\delta$ is the percent deflection and it should less than 40% with a shape factor less than 1.2 for the expected fatigue life of the isolator to be in excess of 1 million cycles.

3.8 Data analysis plan

The vibration emission on the handle, hand, forearm, and arm were recorded via the triaxial accelerometer and IMUs. To evaluate the emission, a calculation based on the ISO 5349-1 standard was used. The ISO standard required that the measured acceleration be weighted and analyzed in a one-third octave spectrum. The frequency weighting was defined mathematically as a realizable filter characteristic, designated Wh. Band-limiting filters were also defined with cut-off frequencies of 6.3 Hz and 1250 Hz. *Figure 16* shows the weighting factor as a function of frequency.

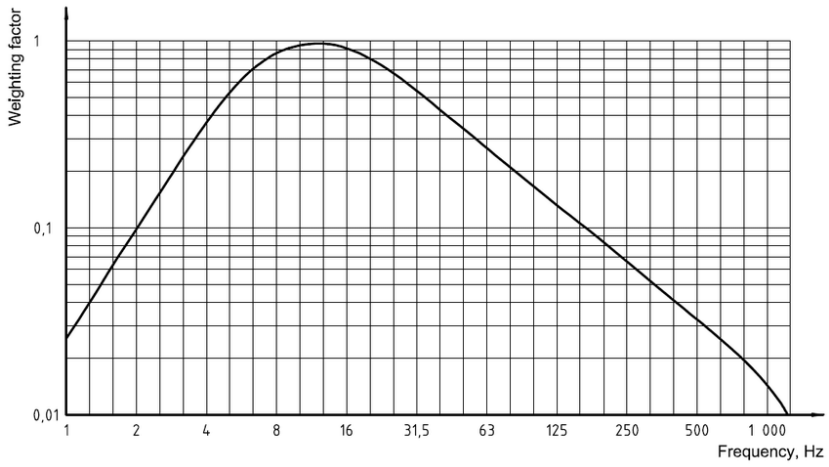

Figure 16: Frequency-weighting-Wh-with-band-limiting-ISO-5349-1.

The ISO 5349-1 standard recognizes the fact that the vibration characteristics of some power tool types are not dominated by a single directional component. Therefore, the root-sum-of-squares of the three frequency-weighted root-mean-square components was calculated using equation 24.

$$a_{hv} = \sqrt{a_{hwx}^2 + a_{hwy}^2 + a_{hwz}^2} \quad (24)$$

Where a_{hv} is the vibration total value and is defined as the root-sum-of-squares of the three component values.

To calculate the vibration total value, only the riveting time is taken into consideration without any of the down time. After finding the vibration total value of each riveting session, the mean value will be calculated as well as the standard deviation in order to check how accurate and reliable the data is.

Raw data of the HavWear was processed through the product's transfer function which is based on the 5349-1 standard. Data is presented as a single root-mean-squared vibration value associated with each tool and it's given in meters per second squared.

For hand-arm vibration a daily exposure should be calculated using equation 25 below:

$$A(8) = a_{hv}\sqrt{\frac{T}{T_0}} \quad (25)$$

Where T is the total daily duration of exposure to the vibration and T_0 is a reference duration of 8 hours (28,800 s).

Chapter IV – Results

4.1 Bucking bar handle design results

The new handle has an overall length of 5” and a diameter of 2”. Using the equations for vibration isolation, the Sorbothane, placed inside the handle, was made of 70-durometer polymer (based on “00” scale) and was designed to be 1” thick with a 1.38” diameter. It is supposed to provide 71.7% isolation. As for the cover, and using the equations for shock isolation, the polymer that was supposed to be used should have been made of 30-durometer and has a thickness of 0.42”. Due to time constraints, a higher durometer handle cover was manufactured and used instead.

4.2 Bucking bar system parameters results

The following section investigates the results from the experiments done on the bucking bar system in order to identify the system’s parameters. *Figure 17* illustrates the spring’s deflection under loading.

1. Spring rate

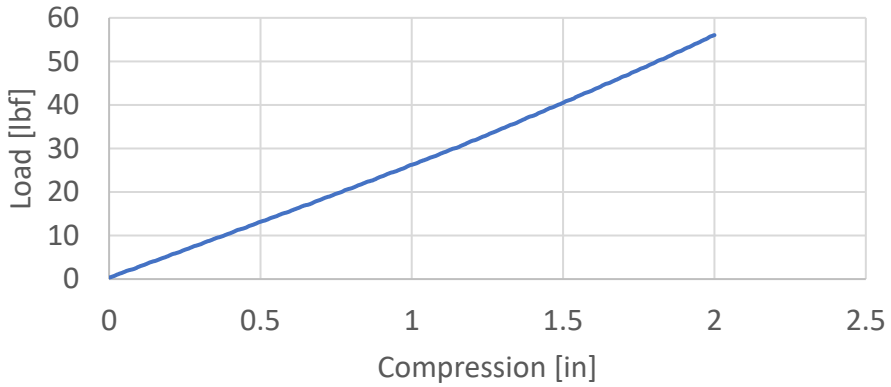

Figure 17: The spring compression versus the load. A spring constant K = 26.53 lbf/in.

Using equation 1, the spring rate was calculated to be $K = 26.53 \frac{lbf}{in} = 4646 \frac{N}{m}$.

2. Hysteresis

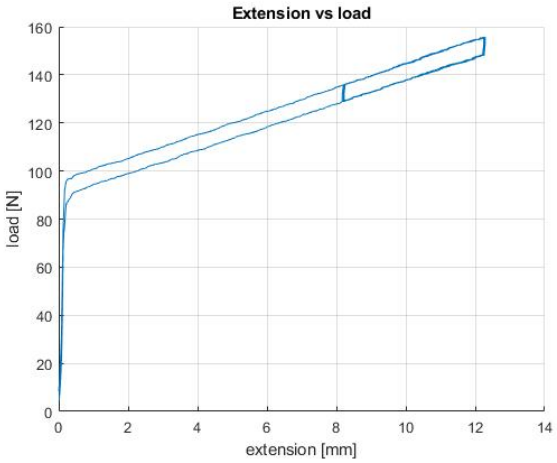

Figure 18: Hysteresis loop recorded on the Instron machine.

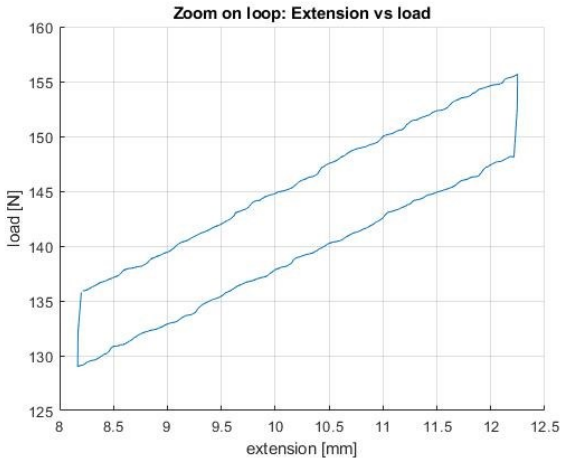

Figure 19: Zoom-in on one hysteresis loop.

By finding the area inside the loop and using equation 2, the friction force was approximated to be $F_c = 3\ N$.

3. Step input

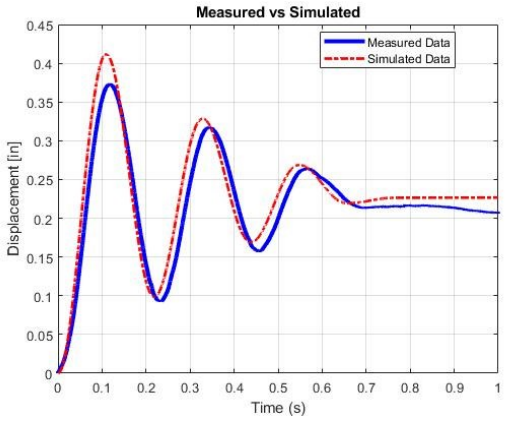

Figure 20: Free response of the bucking bar after a step input.

Using *Figure 20* and equations 3 and 4, and taking into consideration the initial displacement, the viscous damping coefficient was calculated to be $c = 17.22 \frac{Ns}{m}$. Using the calculated spring rate, the calculated damping, and the calculated friction, a step input was simulated as seen in *Figure 20*. The RMSD was calculated to be 6.48% which is less than 10% which means that the model is valid.

4. Impulse input

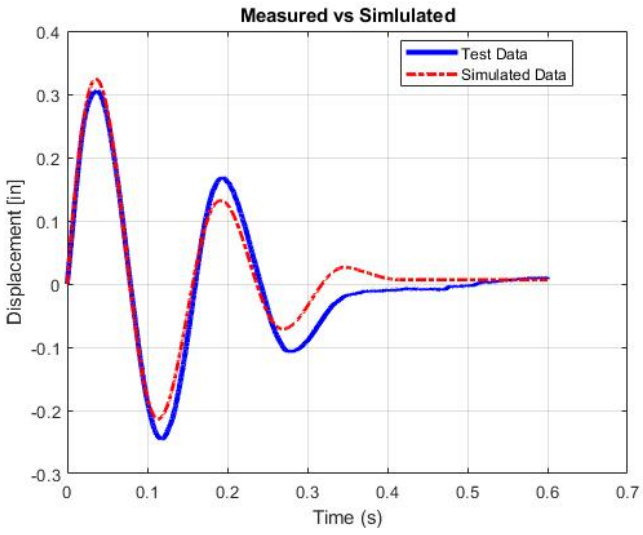

Figure 21: Free response of the bucking bar after an impulse input.

Using *Figure 21* and equations 4 and 5, and taking into consideration the initial displacement, the viscous damping coefficient was calculated to be $c = 10.75 \frac{Ns}{m}$. Using the calculated spring rate, the calculated damping, and the calculated friction, a step input was simulated as seen in *Figure 21*. The RMSD was calculated to be 4.89% which is less than 10% which means that the model is valid.

5. Rivet gun

The measured force on the ICP Force sensor is shown in *Figure 22* below. There was a disconnection during the data acquisition and that hit was disregarded. The average peak force was found to be 3395 ± 538 lbf with a frequency of approximately 26-27 Hz.

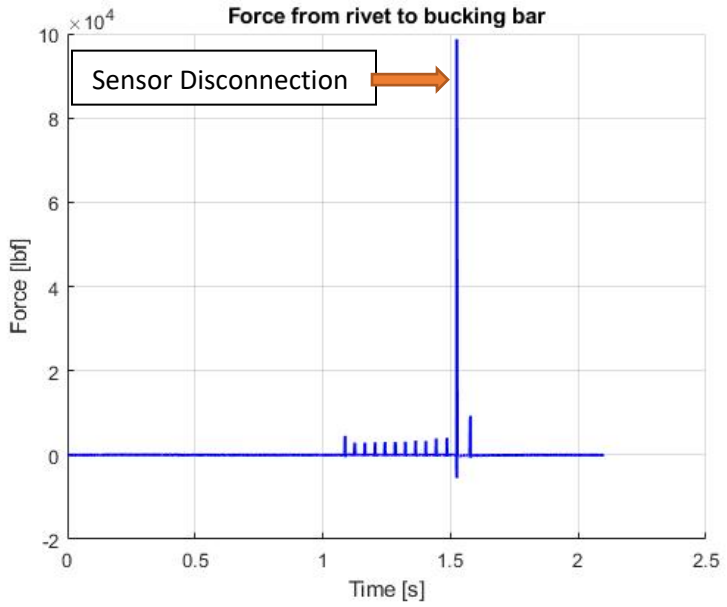

Figure 22: Measured force on the load cell from the rivet during riveting.

6. Rivet

The exact rivet material is Aluminum 7050-T73. The stress strain curve was found in the Atlas of Stress Strain Curves, 2002. The constant $n = 27$ was noted and the constant k was approximated from the plastic region $k = 1.8438 * 10^{56}$.

7. Simulink simulation

    a. Bucking bar's displacement

In order to model the system, a Simulink model was developed, and the parameters calculated earlier were used to simulate the bucking bar. A detailed model is shown in Appendix B. The rivet's information was plugged in as well as the gun's force. *Figure 23* shows the bucking bar's displacement during actual riveting and the simulated riveting using the Simulink model.

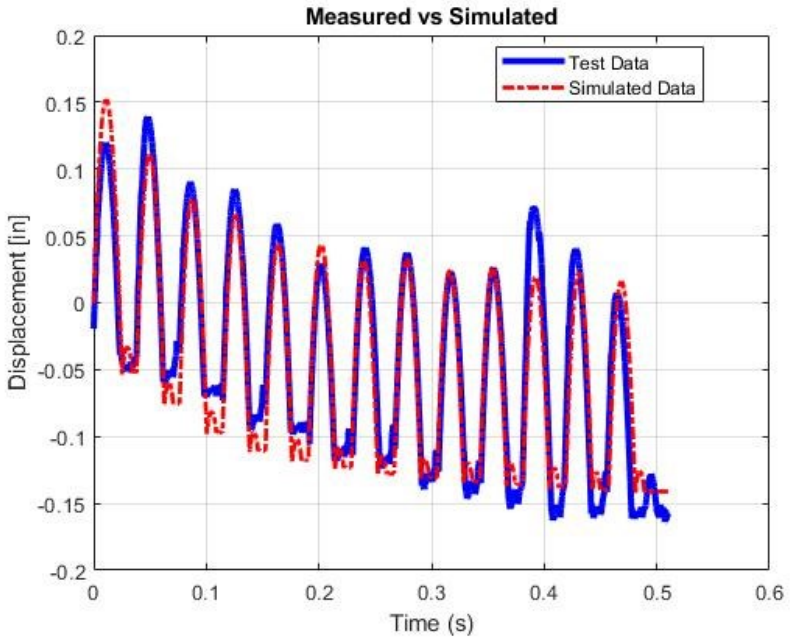

Figure 23: Bucking's bar displacement during actual riveting and the simulated response.

Using the calculated spring rate $k = 4646\frac{N}{m}$, the approximated damping in the horizontal position $c = 30\ \frac{Ns}{m}$, and the approximated friction in the horizontal position

$F_r = 4\ N$, a Simulink model was generated. The RMSD was calculated to be 7.74% which is less than 10% which implies that the model is robust.

b. Rivet's formation

After each hit, the rivet's formation was recorded and compared to the simulated results. *Figure 24* illustrates the rivet's tail height during an experiment and the simulated results, and an average difference of 13.54% was calculated. Given the assumptions made, the model shows a final rivet formation of 0.1411" which yields to a rivet diameter of 0.3443" which puts it within spec (final diameter 0.33" - 0.4").

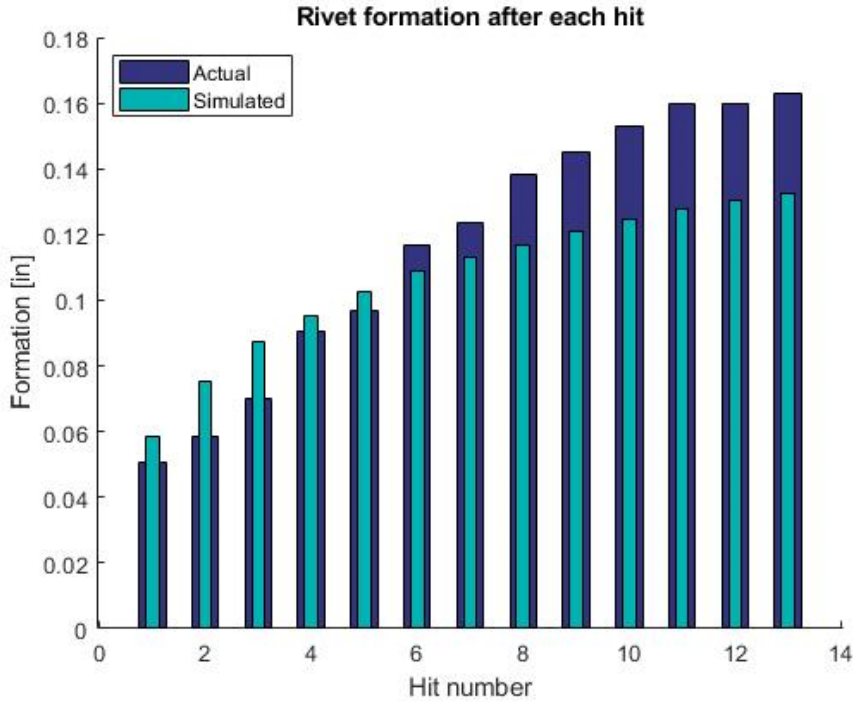

Figure 24: Rivet tail height after each hit.

c. Bucking bar's acceleration

During the actual experiment, an single axis shock accelerometer attached to the bucking bar measured an average peak acceleration of 782 ± 114 g's. As the rivet was being formed, it became stiffer which resulted in higher accelerations with time. Also, the rivet and coupon could oscillate which resulted in smaller accelerations when the bar hits the rivet.

The Simulink modeled the rivet as a fixed hard stop with constant damping and stiffness. This model resulted in a constant peak acceleration of 541 g's throughout the riveting session. Also, the model resulted in higher accelerations when the bucking bar recoiled off the rivet between the rivet gun's hits. Figure *25* below compare the test data collected from the shock accelerometer to the simulated data.

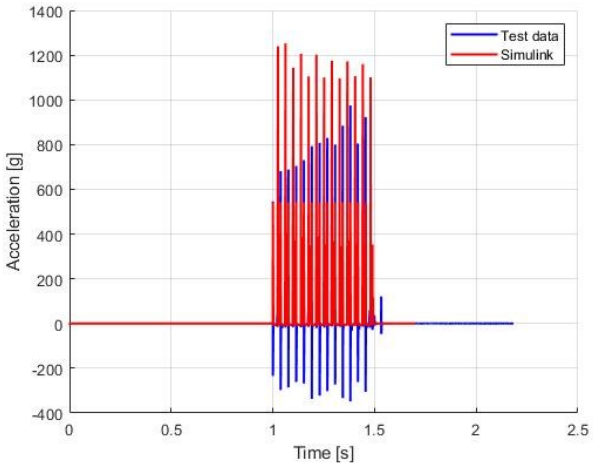

Figure 25: Comparison of the actual bar's acceleration vs the simulated Model.

4.3 Test Bench Results

Vibration emission at the tool's handle recorded via Triaxial Accelerometer

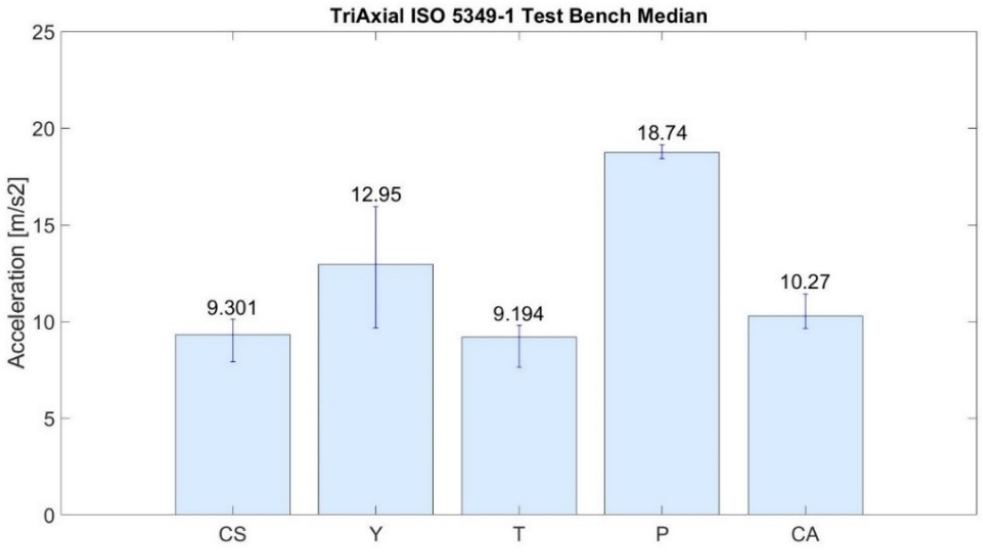

Figure 26: Acceleration emission measured at the tool and weighted according to ISO 5349-1. The values shown are the median RMS values with the 25th and 75th percentile.

As expected, the fixed plastic handle (P) experiences the most vibration emission. All the other handles are spring dampened, and they all showed a reduction in vibration.

Frequency analysis at the tool's handle recorded via Triaxial Accelerometer

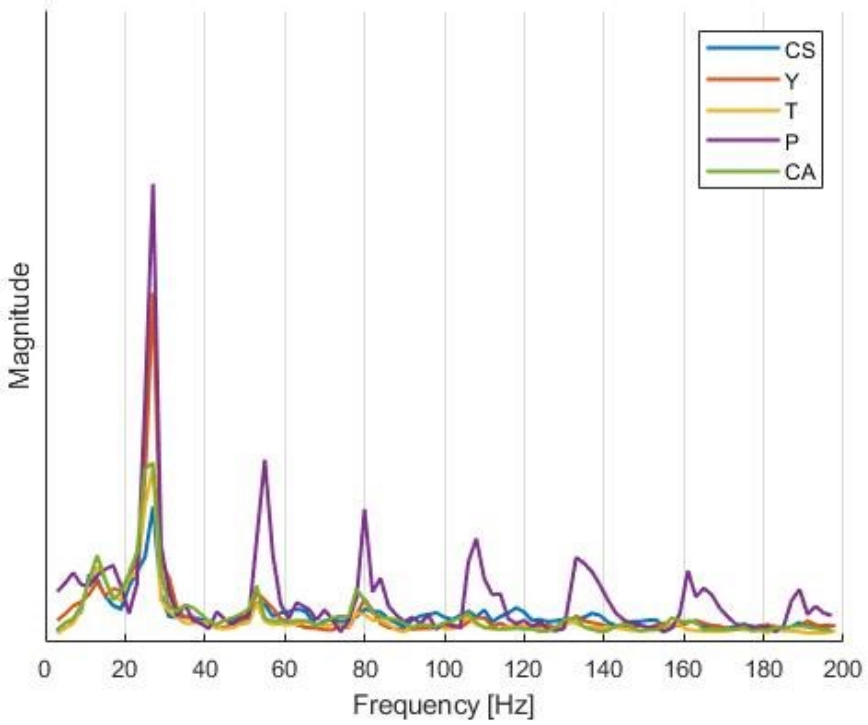

Figure 27: The amount of vibration of each tool at each frequency.

On the test bench, all handles emit the most vibration emission at 26-27 Hz which is the frequency of the rivet gun. The spring loaded handles have almost no energy in the frequencies higher than 80 Hz while the fixed plastic handle still emits energy at the higher harmonics of 26-27 Hz that are higher than 80 Hz.

Rivet Diameter

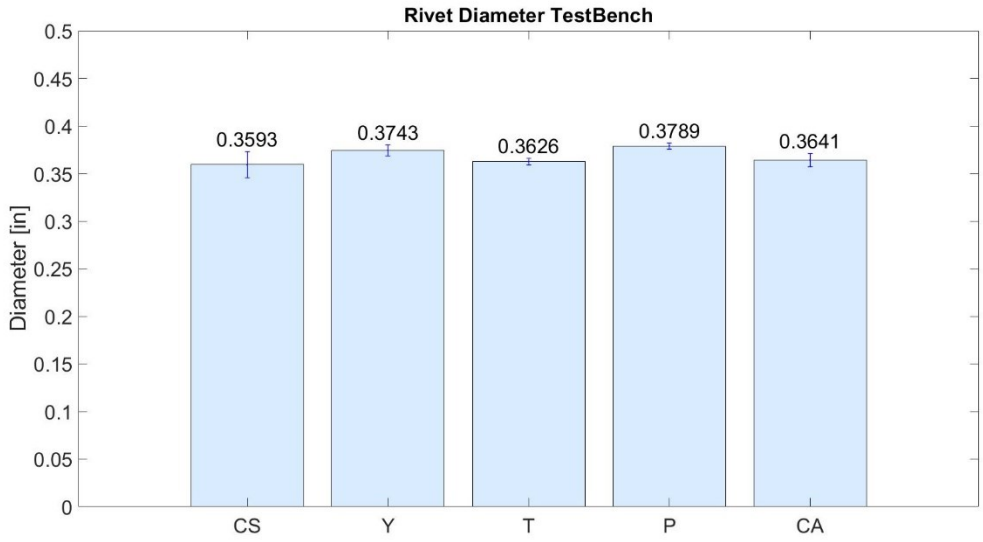

Figure 28: Final Rivet Diameter for each handle. The values shown are the mean diameters values with the standard deviation.

All handles were able to install well-formed rivets that were within specification (final diameter 0.33”-0.4”). There is no significant advantage in using one handle over the other in terms of rivet formation rate.

4.4 Manual Results

Vibration emission at the tool's handle recorded via Triaxial Accelerometer

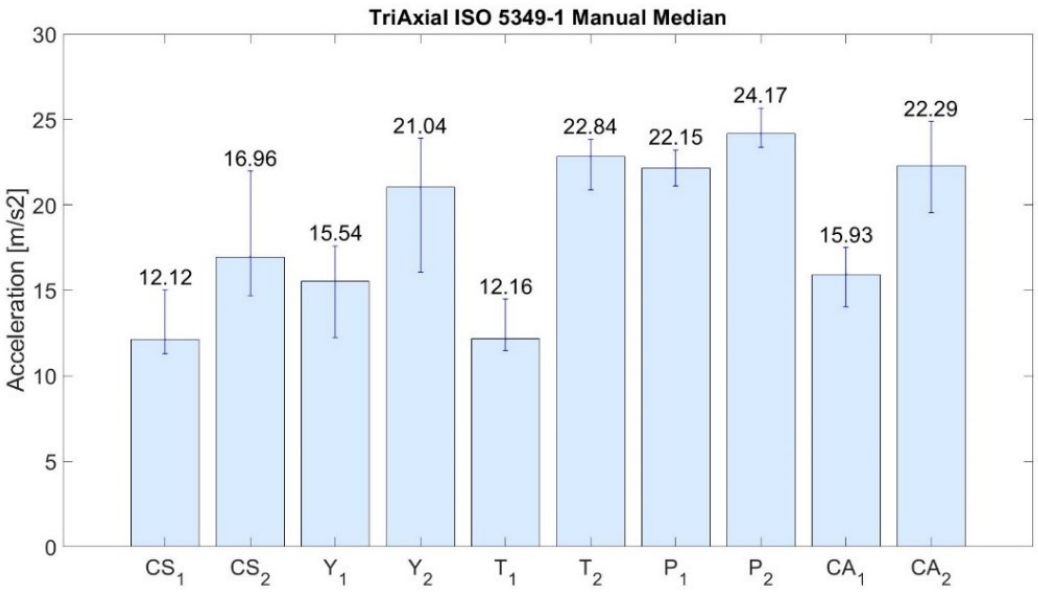

Figure 29: Acceleration emission measured at the tool and weighted according to ISO 5349-1. The values shown are the median RMS values with the 25th and 75th percentile

As expected, the fixed plastic handle emitted the most vibration for both mechanics, while the spring loaded handles isolated some of the vibrations. From the graph it can be seen that mechanic 2 always experiences higher emission while using the same handle as mechanic 1.

Vibration emission on the Mechanic's wrist recorded via HavWear

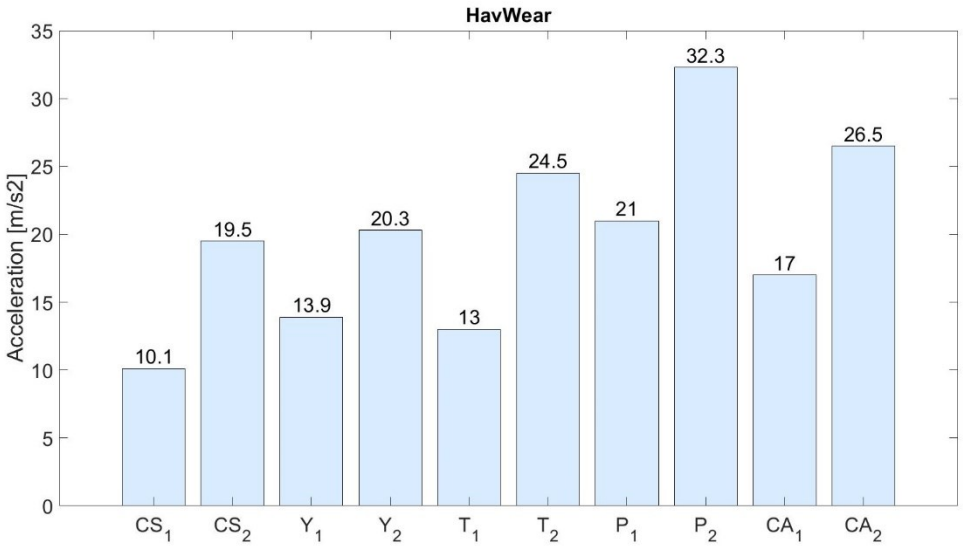

Figure 30: Acceleration emission measured at the mechanics' wrists.

Both mechanics are exposed to the most vibration while they were using the fixed plastic handle. Again, it is seen that mechanic 2 always has higher vibration emission than mechanic 1.

Vibration emission on the Mechanics' operating side recorded via IMUs

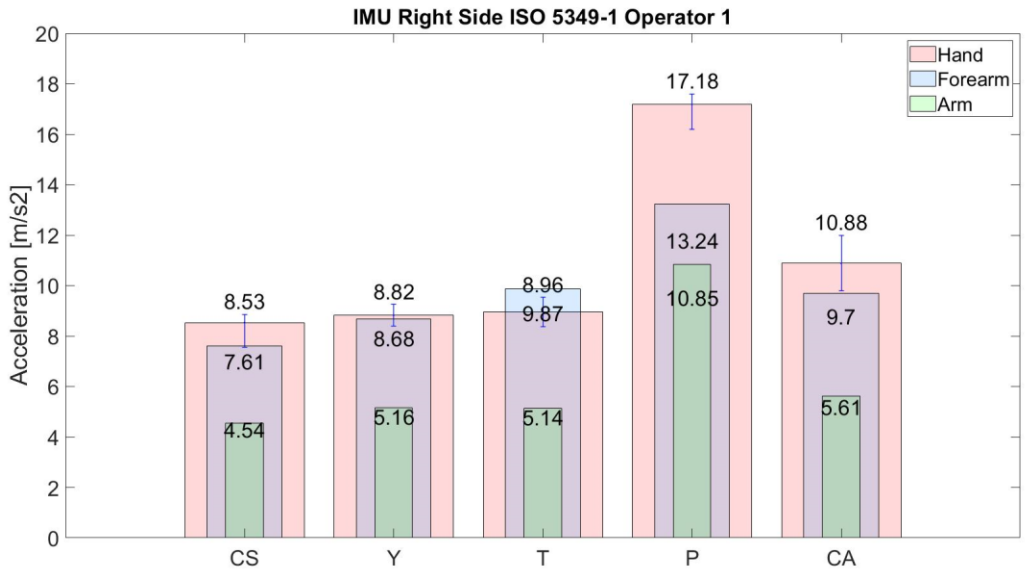

Figure 31: Vibration emission recorded via IMU on the mechanic's right side.

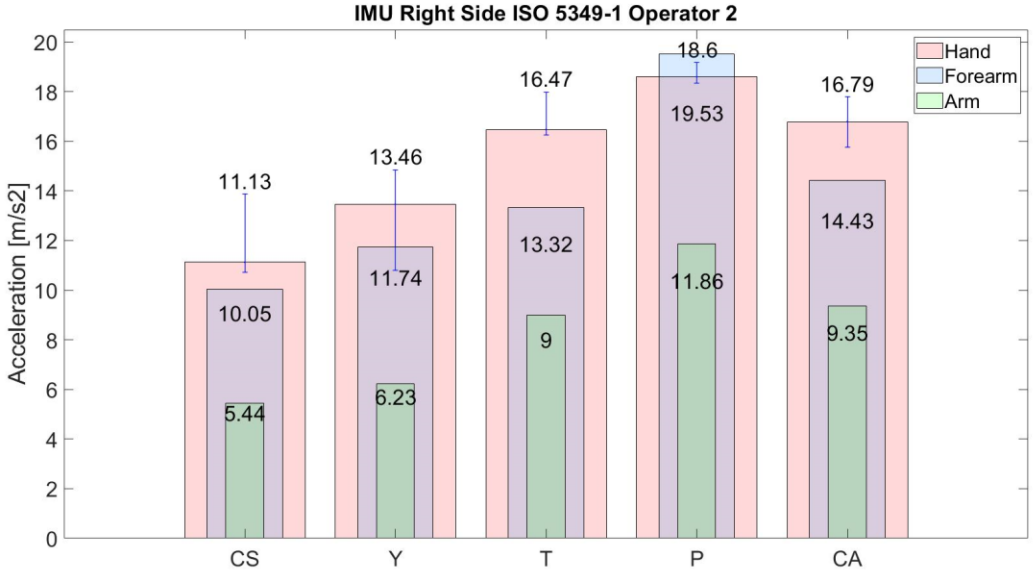

Figure 32: Vibration emission recorded via IMU on the mechanic's right side.

The plastic handle shows the most vibration emission on all parts of the hand-arm system (hand, forearm, and arm). From the graph it can be seen how the acceleration's magnitude gets attenuated as it is traveling from the hand to the arm.

Frequency analysis at the tool's handle recorded via Triaxial Accelerometer

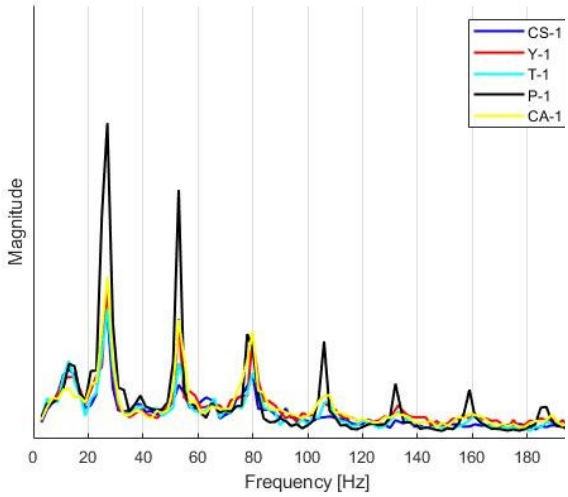

Figure 33: The amount of vibration measured from each handle as a function for Mechanic 1.

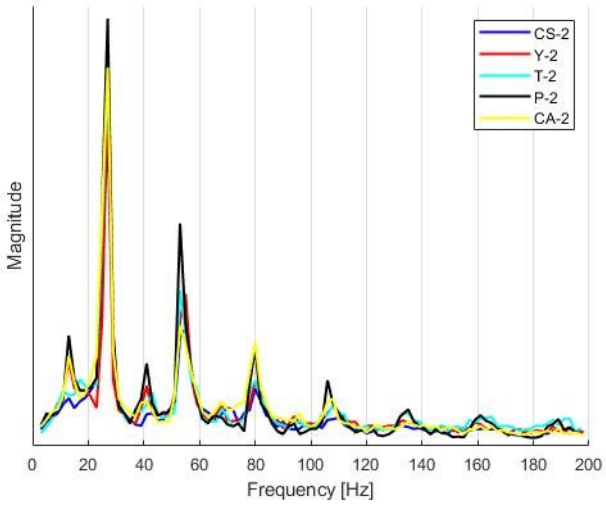

Figure 34: The amount of vibration measured from each handle as a function for Mechanic 2.

For both mechanics, all handles have the most vibration emission at 26-27 Hz which is the frequency of the rivet gun. The spring dampened handles show no frequency content at frequencies higher than 80 Hz. As the frequencies get higher, the energy of the acceleration gets smaller until it diminishes for the frequencies higher than 200 Hz.

Frequency analysis on the Mechanic's body recorded via IMUs

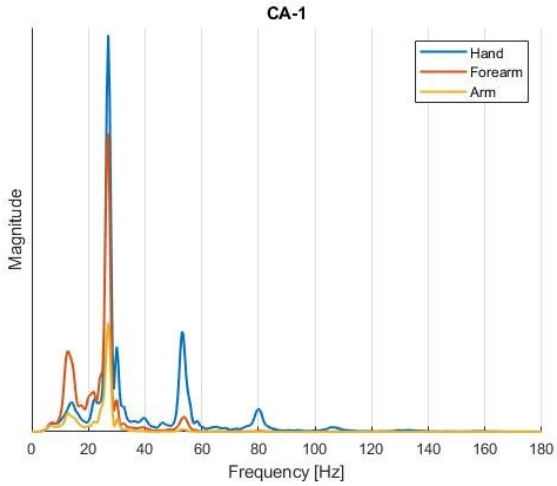

Figure 35: Amount of vibration at each frequency for M1 while using CA.

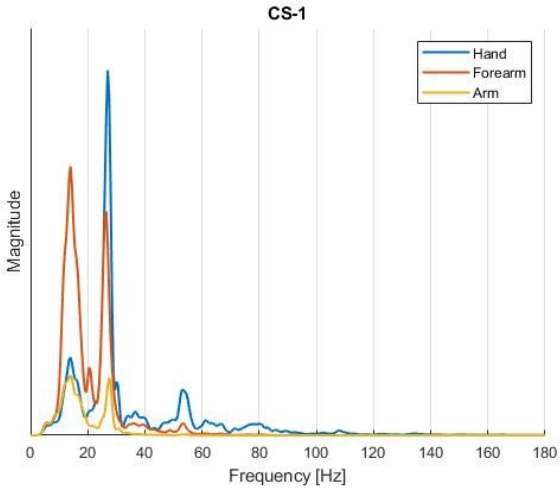

Figure 37: Amount of vibration at each frequency for M1 while using CS.

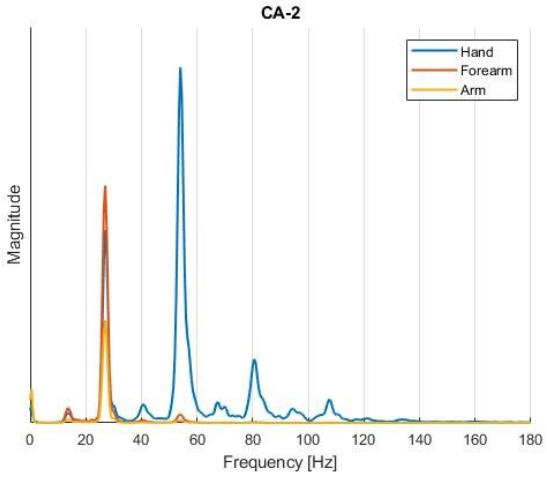

Figure 36: Amount of vibration at each frequency for M2 while using CA.

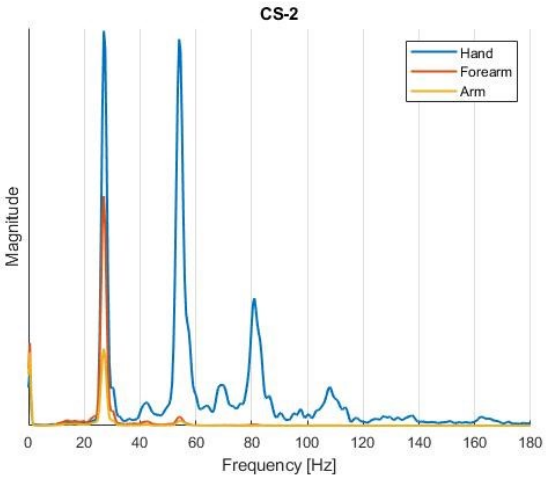

Figure 38: Amount of vibration at each frequency for M2 while using CS.

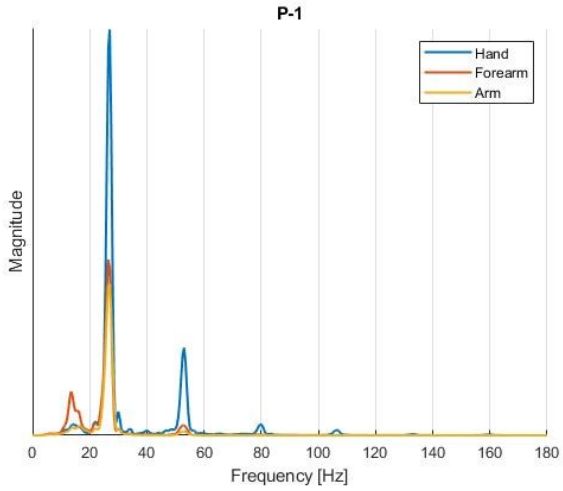

Figure 39: Amount of vibration at each frequency for M1 while using P.

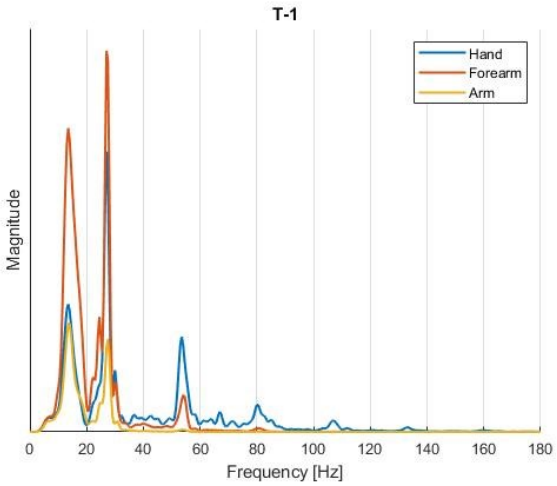

Figure 41: Amount of vibration at each frequency for M1 while using T.

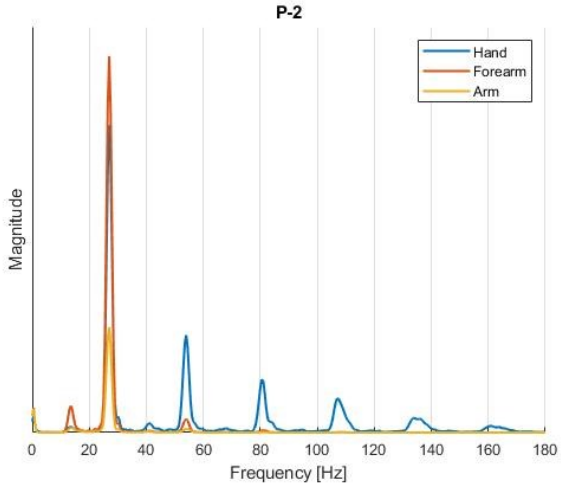

Figure 40: Amount of vibration at each frequency for M2 while using P.

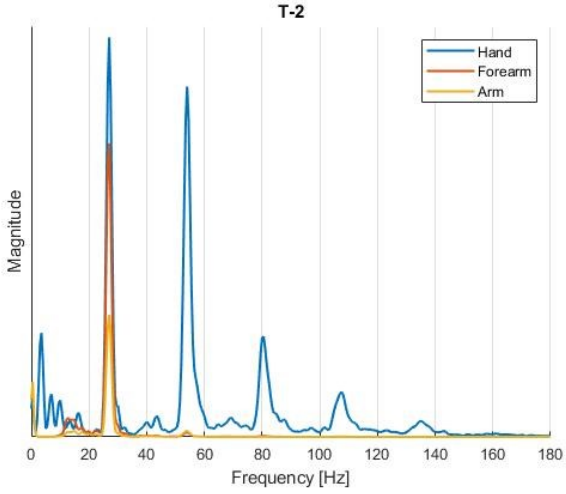

Figure 42: Amount of vibration at each frequency for M2 while using T.

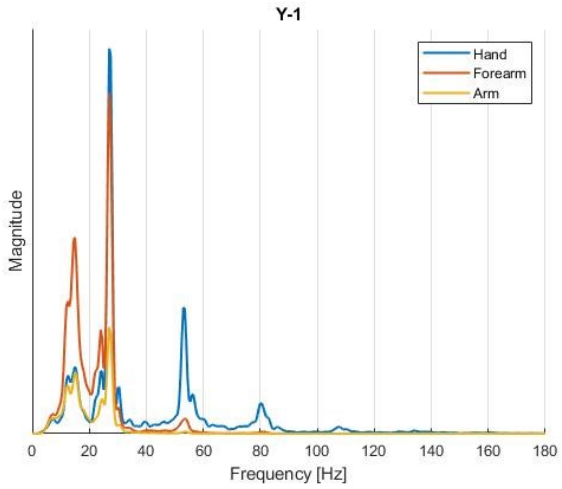

Figure 43: Amount of vibration at each frequency for M1 while using Y.

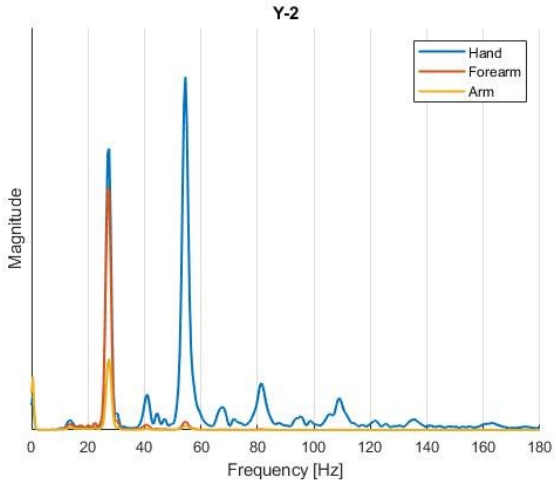

Figure 44: Amount of vibration at each frequency for M2 while using Y.

As expected, the dominant frequency was the frequency of the rivet gun 26-27 Hz. For mechanic 1, some energy content was seen at 13-14 Hz which is half of the driving frequency. Mechanic 2 experience equal or higher vibration emission at the second harmonic of 26-27 Hz.

Rivet Diameter

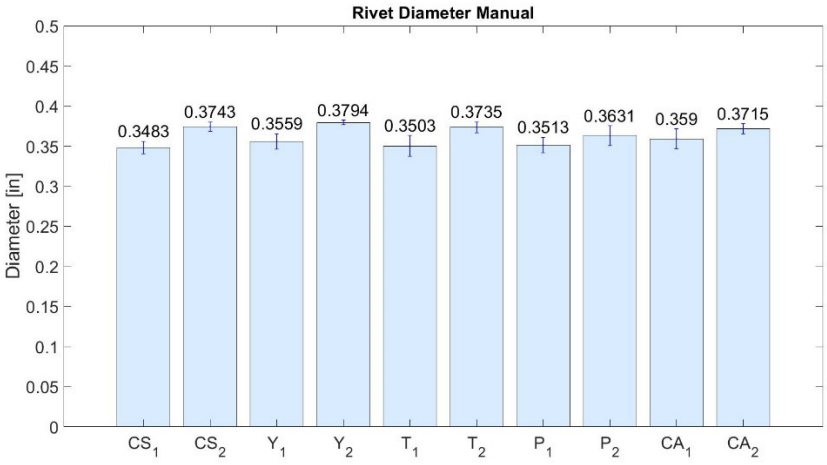

Figure 45: Final Rivet Diameter for each handle and mechanic.

Both mechanics were able to install well-formed rivets that were within specification while using any handle. The two operators were very consistent as the rivets they installed almost had the same average diameter, but riveter 2 always had a larger final diameter.

4.5 Survey results – Mechanics' feedback

After using each tool, the mechanics were asked to answer a set questions discussed earlier in the methods section. The operators would rate each question on a 1-7 scale where 1 is strongly disagree and 7 is strongly agree. *Table 3* and *Table 4* summarize the scores of mechanic 1 and mechanic 2 respectively. For questions 4 and 9, the question would be negating itself (had a reverse order scale) so 8 was subtracted from the score that the mechanics provided to make those questions scales correspond to the other questions.

Table 3: Mechanic 1's answers to the survey question after using each tool.

Question	Tool	P	Y	CA	CS	T
1		2	2	2	3	3
2		2	2	3	1	5
3		3	4	2	3	3
4		4	4	3	5	5
5		3	2	2	2	3
6		3	3	3	4	3
7		3	4	3	3	4
8		5	4	3	5	4
9		2	3	3	5	5
10		2	4	3	6	4

Table 4: Mechanic 2's answers to the survey question after using each tool.

Question	Tool	P	Y	CA	CS	T
1		4	6	6	4	6
2		2	6	6	3	3
3		3	5	5	3	4
4		4	6	6	5	5
5		5	4	5	2	4
6		5	5	6	4	4
7		4	5	6	3	5
8		1	7	6	5	6
9		7	6	6	5	6
10		2	5	4	2	2

Chapter V – Discussion

5.1 Bucking bar handle design

The transmissibility graph shown in *Figure 65* in Appendix D, was used to calculate the Y handle's expected transmissibility of $T_e = 0.09$. *Table 8* in appendix D compares the absolute acceleration recorded on the bucking bar to the absolute unweighted acceleration recorded on the handle. From the table it is concluded that the transmissibility actually is $T_r = 0.1044$, which is a really good approximation of what is expected.

As for the T handle, it was assumed that it had the same amount of friction and damping because the same material is being used. The new handle design has a stiffer spring rate which leads to a transmissibility of $T_e = 0.18$. *Table 9* in Appendix D shows a recorded transmissibility of $T_r = 0.0918$. Then the expected vibration emission would be $V_e = 183.5\ g$ while the recorded one was $V_r = 93.6\ g$ which leads to a 64.88% difference. That means that the damping material provided an additional 65% isolation which agrees with the expected 71.68% isolation with a 9.96% difference.

5.2 Operator 1 vs Operator 2

Using the fixed plastic handle both mechanics experienced almost the same amount of vibration emission. When using the spring loaded handles, subject 2 always experienced more vibrations than subject 1. Operator 2 was smaller in size and weighs much less than operator 1. He also mentioned that he pushed more on the bar to get it in its spot before the riveting starts while the other mechanic just held the bar against

the rivet without applying much force. This harder pushing was supported by the fact that the diameter of the rivets that mechanic 2 installed were always greater than the ones installed by the first mechanic. Therefore, it can be concluded that operator 2 had more coupling with the tool and he weighs less, which could explain the higher vibration experienced by him.

5.3 Vibration emission at the tool's handle – Triaxial

The data recorded via the triaxial accelerometer on the tool's handle was consistent between the automated and the manual testing. Both sets of data showed the same trend in vibration emission of the different handles.

On the test bench the plastic handle performed the worst in terms of vibration emission. Its root-mean-squared value of the weighted acceleration is 18.74 $\frac{m}{s^2}$ which was double the value of the handle that experienced the least vibration emission. *Figure 46* below shows the percent difference between the vibration emissions of each handle compared to the plastic handle. A positive value indicates less emission, so a better handle and a negative value means that the handle emits more vibration.

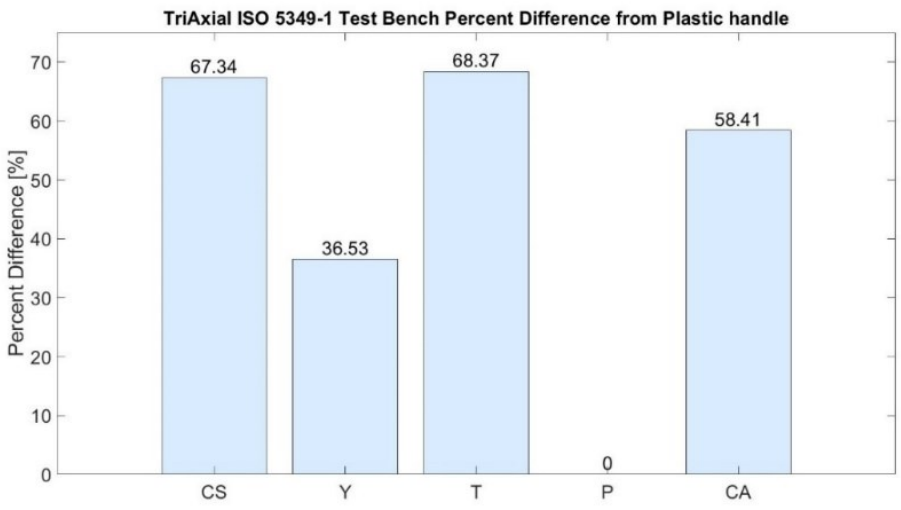

Figure 46: Percent difference between the vibration emission of each handle compared to the plastic one on the test bench.

From the graph it can be noted that all handles performed better than the fixed plastic one and the T handle with the damping material reduced the vibrations the most and by 68.37% on the test bench.

As for the manual installation, mechanic 2 always experienced higher vibrations with all of the handles. While using the plastic handle, both mechanics experienced the worst vibration emission and the spring handles always showed some sort of vibration reduction. *Figure 47* shows the percent difference between the vibration at the tool's handle compared to the plastic one.

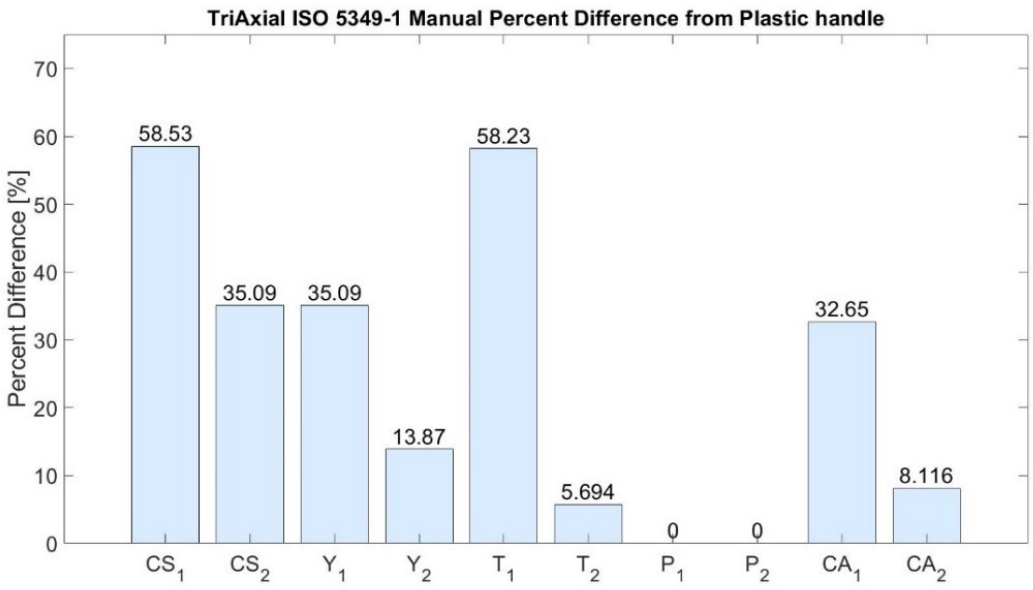

Figure 47: Percent difference between the vibration emission of each handle compared to the plastic one during manual testing.

From the graph it can be seen that the first operator experienced significantly less vibrations while using the spring handles. The vibrations were reduced by 32-35% while using the CA and the Y handles and by 58% when using the CS and the T handles. This significant reduction may be due to less coupling between the operator and the spring loaded handles.

Mechanic 2 also experienced less vibrations while using the spring load handles, but the reductions weren't as significant as the ones for the first operator. The T handle with the damping material and the CA one only reduced the vibrations by 5.7% and 8.1% respectively. The CS handle reduced the vibration the most and by 35% while the Y one fell in between all the other ones with a reduction of almost 14%.

In order for the spring loaded handles to be effective, less coupling with the tool would be desirable. The mechanics should be trained on how to properly use this tool in for them to benefit the most from their designs.

5.4 Vibration emission at the wrist – HavWear

The data recorded via the wrist-mounted HavWear sensors estimating the operator's vibration exposures experienced at the right hand wrist was consistent with the data recorded at the tool's handle. The values for both mechanics follow the same trend and show that the fixed plastic handle (P) was the worst in terms of vibration emission. *Figure 48* compares the HavWear sensed vibration at the wrist while using each handle relative to plastic handle.

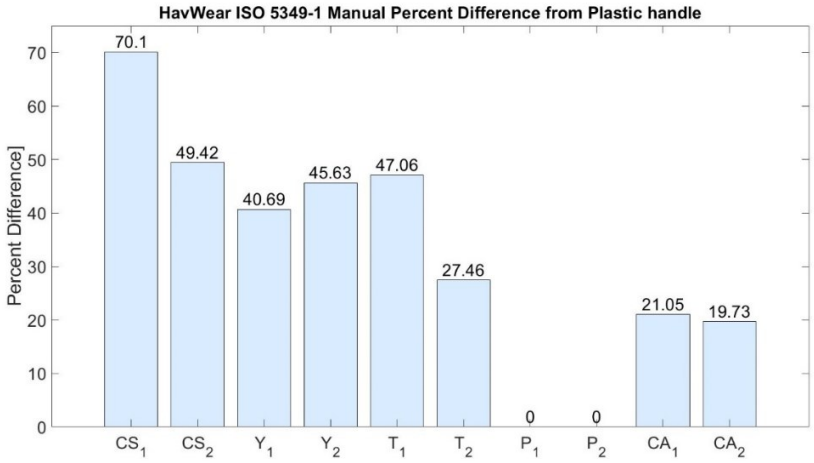

Figure 48: Percent difference between the vibration emission of each handle compared to the plastic one during manual testing.

Based on the HavWear data, the CS handle reduced the vibration emission the most for both mechanic 1 (70.1%) and mechanic 2 (49.4%) while the CA one reduced it

the least and by almost 20%. Those results are consistent with what was measured by the triaxial accelerometer on the tool's handle.

5.5 Vibration emission on the mechanics' operating side – IMU

The data recorded via the IMUs accelerometers on the mechanics' right hand, forearm, and arm were compared with the data recorded on the tool's handle. Both sets of data showed the same trend in vibration emission of the different handles.

Mechanic 2 and while using the same handle as mechanic 1 always experienced higher vibrations at all locations. For both mechanics the CS handle was the best in terms of vibration emission as it reduced the vibration on the hand by 67% for mechanic 1 and by 50% for mechanic 2. *Figure 49* compares the vibration at the hand while using each handle relative to plastic one.

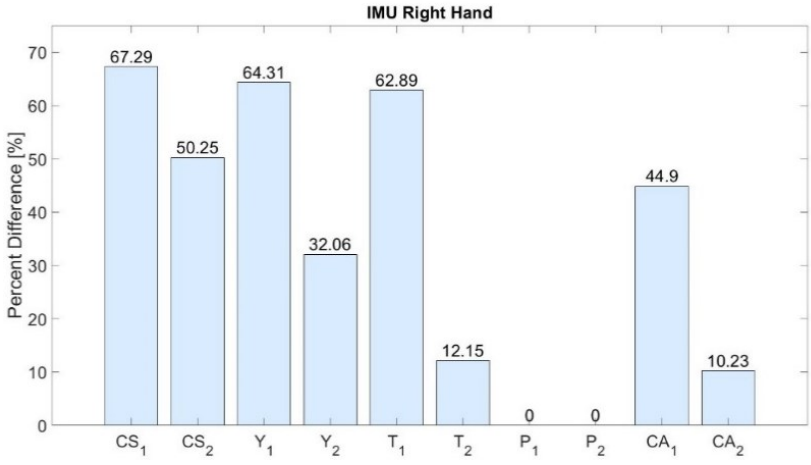

Figure 49: Comparison of the vibration emission of both mechanics at the hand level. Mechanic 1 experiences better vibration isolation. The CS handle shows the best vibration reduction.

While using the spring dampened handles mechanic 1 experiences on average a vibration reduction of 52% across all handles, while mechanic 2 only experiences a reduction of 26% at the hand level.

Figure 50 below compares the vibration emission at the mechanics' forearm relative to the fixed plastic handle.

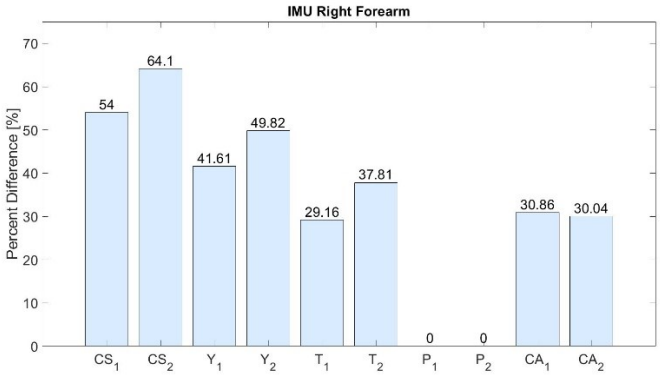

Figure 50: Comparison of the vibration emission of both mechanics at the forearm level. Mechanic 2 experiences better vibration isolation. The CS handle shows the best vibration reduction.

At the forearm level, the CS handle was the best for both mechanics as it reduced the vibration the most and by 54% and 64.1% for mechanic 1 and 2 respectively. Operator 2 experienced higher vibration reduction which is not what is seen on the hand and wrist. While using the spring loaded handles and on average, operator 1 saw a reduction of 38.9% and operator 2 experienced a 45.4% reduction.

Figure 51 shows the vibration emission at the mechanics' arm relative to the fixed plastic handle.

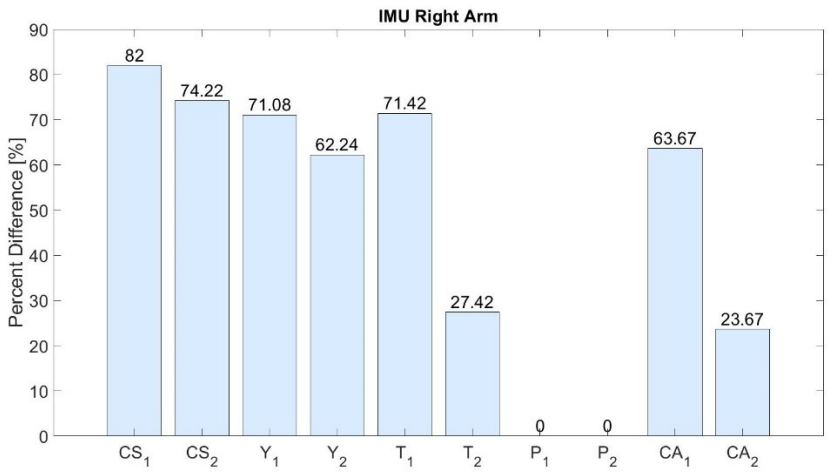

Figure 51: Comparison of the vibration emission of both mechanics at the arm level. Mechanic 2 experiences better vibration isolation. The CS handle shows the best vibration reduction.

At the arm and while using the spring dampened handles, 72% of the vibration magnitude is dissipated for mechanic 2. As for the first mechanic, he also saw a large reduction of 68% when using the CS and Y handles, but with the T and CA he only experienced a 25% reduction.

5.6 Vibration emission from handle-hand-forearm-arm

Using the data from all sensors, an analysis on how the vibration propagates in the human hand-arm system was done. *Table 5* and *Table 6* below show the percentage of the remaining vibration magnitude at each location for each handle and mechanic. They compare the remaining percentage between the value at a specific location compared the value recorded on the tool's handle

Table 5: Vibration attenuation at each location with each handle for mechanic 1.

Operator 1	Handle	Hand	Forearm	Arm
CS	100 %	70.8 %	62.79 %	37.46%
Y	100 %	56.76 %	55.86 %	33.2 %
T	100 %	73.68 %	81.17 %	42.27 %
P	100 %	77.56 %	59.77 %	48.98 %
CA	100 %	68.3 %	60.89 %	35.21 %

Table 6: Vibration attenuation at each location with each handle for mechanic 2.

Operator 2	Handle	Hand	Forearm	Arm
CS	100 %	65.62 %	59.26 %	32 %
Y	100 %	63.97 %	55.8 %	29.61 %
T	100 %	72.11 %	58.32 %	39.4 %
P	100 %	76.95 %	80.8 %	49.07 %
CA	100 %	75.32 %	64.73 %	41.95 %

The tables above show that 73.8% of the vibration reach the hand, 63.94% reach the forearm, and 38.91 % reach the arm. That means that the hand-arm system acts as a vibration dampener and/or low pass filter as the vibration gets smaller and smaller as it is moving through the body.

When using the plastic handle, the remaining vibration at the arm level was the highest with almost 50% still present, while it was in the 30% range for all the other handles.

This demonstrates that different bucking bar handle designs can affect the amount of vibration transmitted to the hand of the bucking bar operator and also into the arm.

5.7 Frequency Analysis

For all handles, most of the vibration energy is present at the gun's frequency which is 26-27 Hz. As the frequencies get higher and at the harmonics of 26-27 Hz, the energy of the vibration gets smaller until is all diminishes after 200 Hz. That may mean that the hand arm system acts as a low pass filter with a cutoff frequency of 200 Hz.

From the graphs it can be seen that the frequencies higher than 40Hz barely reach the forearm and the arm. This means that the forearm and arm acted as a low pass filter with a cutoff frequency around 40Hz.

Some handles experienced some vibration at frequencies of 13-15 Hz and their harmonics. If those energy contents can negatively affect the human health, a way to cut those energies in those frequencies should be investigated.

5.8 Rivet formation

For a rivet to be within specification, its final diameter needs to be 0.33”-0.40”. During both the automated and the manual installations all rivets were well formed and met the specification. There was no bucking bar that showed significant improvement over the other. Therefore, in terms of rivet formation rate, all bucking bar handles performed similarly and any one of them could be used to do the job.

5.9 Test Bench vs Manual- Triaxial Data and rivet formation

The vibration data acquired during the automated testing agreed with the data acquired during the manual installations. Both sets of data have the same trend and on average, the values calculated from the test bench are 26.44% less than the values found during manual testing.

As for the rivet quality, the test bench and the mechanics formed the rivets well and they were all in spec with no bar significantly forming better rivets.

To quantify a handle's performance and have a good approximation of the vibration emission, the test bench serves as a dependable mean of testing.

5.10 Triaxial vs IMU vs HavWear

The data acquired from several sensors agree and follow the same trend. The HavWear data represented a close match for both the vibration measured at the tool's handle as well as at the mechanic's hand. For future testing and with further development of the HavWear sensors, they can be used as a reliable data acquisition method. The ease of use and their tracking system makes them ideal to be implemented on a larger scale. It is recommended to use these sensors on the factory floor in order to have more operators and several different tool types and applications.

5.11 Mechanics' feedback

Table 7 below ranks the handles based on the questions asked and the mechanics' scores. The tools are ranked from best (left) to worst (right).

Table 7: Ranking of the tools based on the mechanics' score.

Easiest tool to use	P	CS	Y, CA	-	T
Most comfortable tool on hands and wrists	P	CS	T, Y	-	CA
Most comfortable tool on arms and shoulders	P	CS	T, CA	-	Y
Hard to make errors with this tool	P	CA	CS, Y	-	T
Liked the weight of the tool	CS	Y	CA, T	-	P
I can quickly complete tasks using this tool	T	CS, Y, P	-	-	CA
I like the overall feel of the tool	CS	P	CA, T, Y	-	-
This tool provided less vibration	P	CA	CS, T	-	Y
I adjusted to this tool quickly	Y, CA, P	-	-	CS	T
I like the handle of this tool	P	T	CA	CS	Y

More subjective questions were asked at the end of the riveting session and are available in Appendix C. It is worth noting that mechanic 1 said the plastic handle is his favorite because he is used to it, and mechanic 2 preferred the CA because of its size, weight, and comfort while using it.

Mechanic 1 pointed that the T handle is his least favorite because of its size and fit in his hand while mechanic 2 didn't like the P handle because it causes to most vibration and fatigue to the body.

Finally, they were asked which tool they would choose to replace the existing tools that use at work and they both said that they would want the CA to replace the P. they also added that the CA should have the same geometry as the P (a dome shaped handle).

Chapter VI – Conclusion and Recommendations

6.1 Simulink Model

The Simulink model was able to predict the bucking bar's displacement with a RMSD = 7.74%. Several areas in the model could be improved upon in order to make the model more realistic. The friction and damping should be looked into to make sure if they are constants or time dependent. The model couldn't predict the bucking bar's acceleration accurately, therefore the rivet should be allowed to have some oscillation instead of being modeled as a hard-stop. Also, the rivet should have an adaptive stiffness and damping as it is being formed. The simulation didn't predict the handle's acceleration accurately so a new way of modeling it should be developed. Finally, the formation after each hit was different between the model and the actual experiment. A closer look into the rivet gun's output should be done.

For developing the Simulink model further, it is recommended that the gun and the coupon should be incorporated. A more advanced version of the model could have a set of coupon thicknesses, rivet types and sizes, and different rivet guns that the user can easily choose from. It should also allow the operator to easily design a mass spring damper system based on the information provided earlier. Ultimately, the Simulink model should be able to suggest an optimal bar mass, spring rate, and damping coefficient.

6.2 Bucking bar handles

Five different bucking bar handles were tested on an automated test bench and then Boeing mechanics used them to form rivets. The results showed that the spring loaded bars reduced the vibration by an average of 57.75% on the test bench compared to the fixed handle. The spring dampened bars showed a mean vibration reduction of 45% for mechanic 1 and of 16% for mechanic 2. There was no advantage of adding a damping material to a spring dampened bar that has a higher spring rate.

This study shows that adding a spring to dampen the vibration reduces the amount of vibration transmitted to the hand through the arm of the operator. Implementing recoilless tools on the factory floor would result in less injuries and in a safer and more ergonomic work environment.

In terms of rivet formation, there was no advantage of using a specific bucking bar handle over the other. On the test bench as well as during the manual testing, all handles were able to install good quality rivets that were all within specification.

For further testing, instead of using the triaxial accelerometer on the tool's handle, having the HavWear on the mechanic's wrist is a good approximation of the vibration emission. The use of HavWear also allows to have more test subjects as well as more tools. It is recommended to use the HavWear sensors on the factory floor to have a broader idea of which tool's the best.

As for the test bench, it was able to mimic the manual riveting in terms of vibration emission as well as rivet formation. The use of the test bench alone should give a really good approximation on the vibration emission of each tool.

Based on the data collected and on the mechanics' feedback, it is recommended to use the CS handle to install fuselage rivets where space is not an issue. This handle is recommended because overall it had the least vibration emission. Further investigation can be done on having a lower spring rate which leads to lower transmissibility, but the bar would become harder to control.

Bibliography

[1] Jorgensen M.J., Viswanathan M. (2005). Ergonomic Field Assessment of Bucking Bars During Riveting Tasks, Proceedings of the Human Factors and Ergonomics Society 49th Annual Meeting, 1354-1358.

[2] Ford B., Mott R., Wavrin L., Zaklit W. (2017). Quantifying effective performance and ergonomic impact of riveting tools and bucking bars at work.

[3] Bureau of Labor Statistics (2015). “nonfatal occupational injuries and illnesses requiring days away from work, 2015. [Online] https://www.bls.gov/news.release/pdf/osh2.pdf. [Accessed, October 2018].

[4] Health surveillance for Hand-Arm vibration syndrome. [Online] http://www.hse.gov.uk/vibration/hav/advicetoemployers/havsemployers.pdf [Accessed, October 2018].

[5] Occupational Health and Safety (2018). “Effects of Vibration”. [Online] http://www.ohsrep.org.au/hazards/vibration/effects-of-vibration. [Accessed, October 2018].

[6] Vibrosense Dynamics (2018). “Hand Arm Vibration Syndrome”. [Online] http://www.vibrosense.eu/knowledge-bank/medical-background/hand-arm-vibration-injuries. [Accessed, October 2018].

[7] Sonya Bylund, Lage Burstrom, Anders Knutsson. (2001). A descriptive study of women injured by Hand-Arm Vibration.

[8] Bovenzi, M. (2011). Hand Transmitted Vibration. [Online]. http://iloencyclopaedia.org/part-vi-16255/vibration/84-50-vibration/hand-transmitted-vibration. [Accessed, October 2018].

[9] Burdorf A., Monster A. (1991). Exposure to vibration and self-reported health complaints of riveters in the aircraft industry, Annals of Occupational Hygiene, 35, 287-298.

[10] Azmir N.A., Ghazali M. I., Yahya M.N., Ali M.H., Song J.I. (2015). Effect of Hand Arm Vibration on the Development of Vibration Induce Disorder among Grass Cutter Workers.

[11] Nilsson T., Wahlstrom J., Burstrom L. (2016). Hand-arm vibration and the risk of vascular and neurological diseases-A systematic review and meta-analysis.

[12] Charles L., Ma C, Burchfiel C, Dong R. (2018). Vibration and Ergonomic Exposures Associated with Musculoskeletal Disorders of the Shoulder and Neck.

[13] Bonvenzi M., Fiorito A., Volpe C. (1987). Bone and joint disorders in the upper extremities of chipping and grinding operators. International Archives of Occupational and Environmental Health, 50, 189-198.

[14] Bovenzi M., Zadini A., Franzinelli A., Borgogni F. (1990). Occupational musculoskeletal disorders in the neck and upper limbs of forestry workers exposed to hand-arm vibration.

[15] Griffin M. J., (1990). Handbook of Human Vibration. Academic Press Limited. London.

[16] Kihlberg S., Hagberg M. (1997). Hand-arm symptoms related to impact and nonimpact hand-held power tools, International Archives of Occupational and, Environmental Health, 69, 282-288.

[17] Hagberg M. (2002). Clinical assessment of musculoskeletal disorders in workers exposed to hand-arm vibration.

[18] Dandanell R., Engstrom K. (1986). Vibration from riveting tools in the frequency range 6 Hz-10Mhz and Raynaud's phenomenon. Scandinavian Journal of Work, Environment and Health, 12, 338-342.

[19] Centers for Disease Control and Prevention. Vibration Syndrome (1983). DHHS (NIOSH) Publication Number 83-110

[20] Taylor W., Pelmear P., Pearson J. (1975). A longitudinal study of Raynaud's Phenomenon in chain saw operators. In: Vibration White Finger in Industry. Taylor W, Pelmear PL, eds. London: Academic Press; 15 – 20.

[21] Troell, E., Lindell, H., Gretarsson L. (2018). Zero vibration injurie achieved by machine redesign.

[22] Lundstrom R. (2018). Vibration Produced by Percussive Hand Tools is an Underestimated Contributor to the Development of Vibration Injury.

[23] Lindell H. (2018). High frequency vibration: measurement, effects on biologic tissue and risk assessment.

[24] Boileau P.E., Scory H., Brooks G., Amram M. (1992). Hand-arm vibration associated with the use of riveting hammers in the aerospace industry and efficiency of `antivibration' devices.

[25] McDowell T., Warren C., Xu X., Welcome D., Dong G. (2005). Laboratory and Workplace Assessments of Rivet Bucking Bar Vibration Emissions

[26] Dale, A.M., Standeven, J., & Evanoff, B. (2006). Comparison of anti-vibration interventions for use with fastening tools in metal, First American Conference on Human Vibration, Morgantown, West Virginia.

[27] Cherng JG., Eksioglu M., Kizilaslan K. (2009). Vibration reduction of pneumatic percussive rivet tools: mechanical and ergonomic re-design approaches.

[28] Spring S. Hull, "Evaluation of ergonomic interventions for bucking bars in aircraft manufacturing." Doctor of Philosophy thesis, Wichita State University, Wichita, KA, 2008.

Appendix A – Sorbothane Design Guide

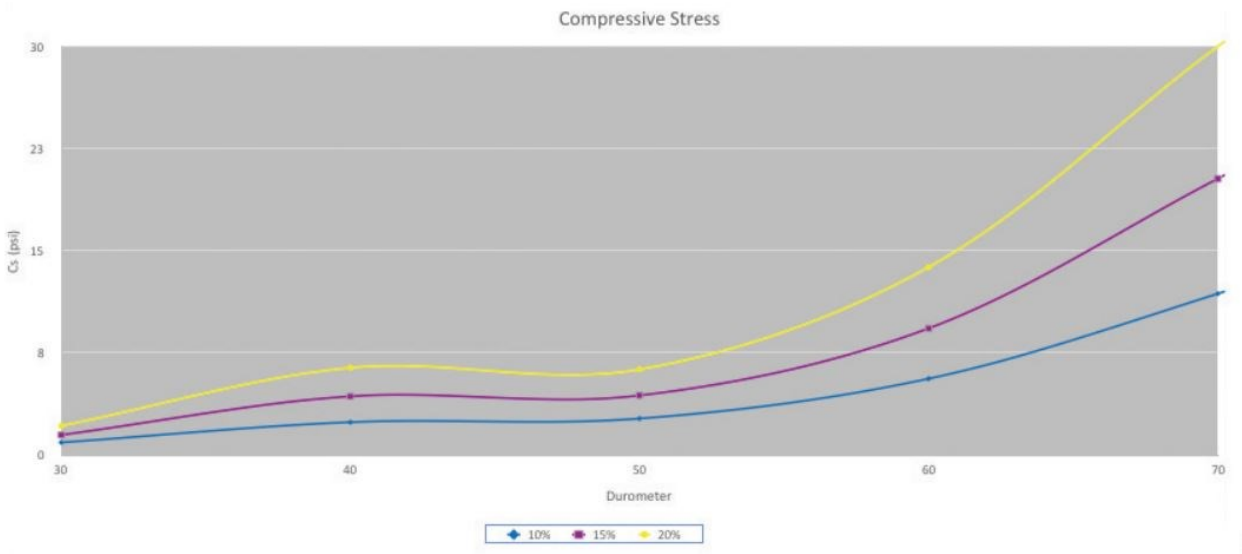

Figure 52: Compressive modulus graph provided by Sorbothane - Engineering Design Guide

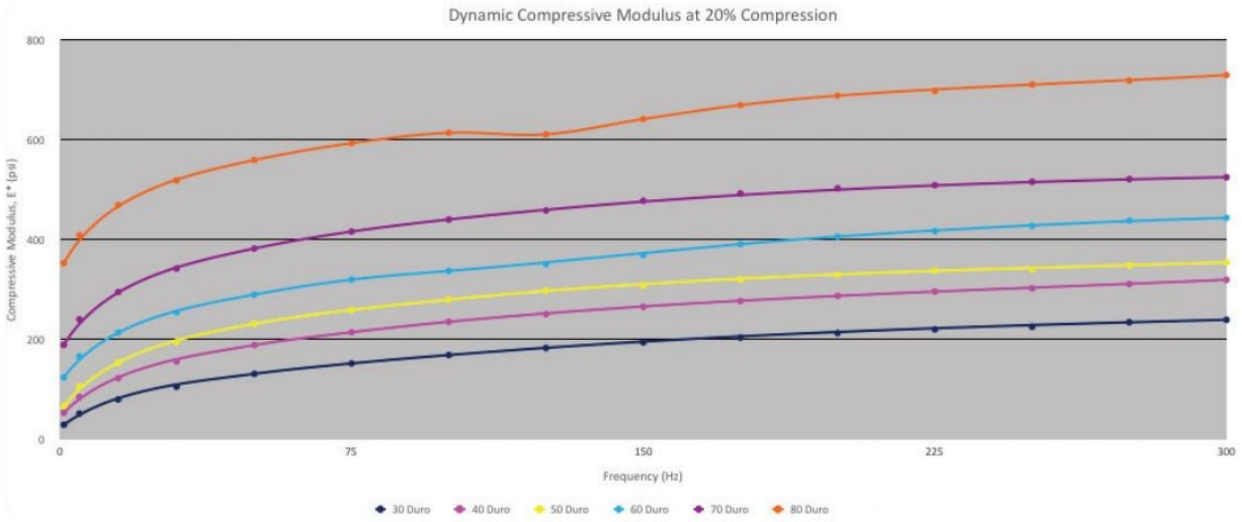

Figure 53: Dynamic Compressive Modulus provided by Sorbothane - Engineering Design Guide

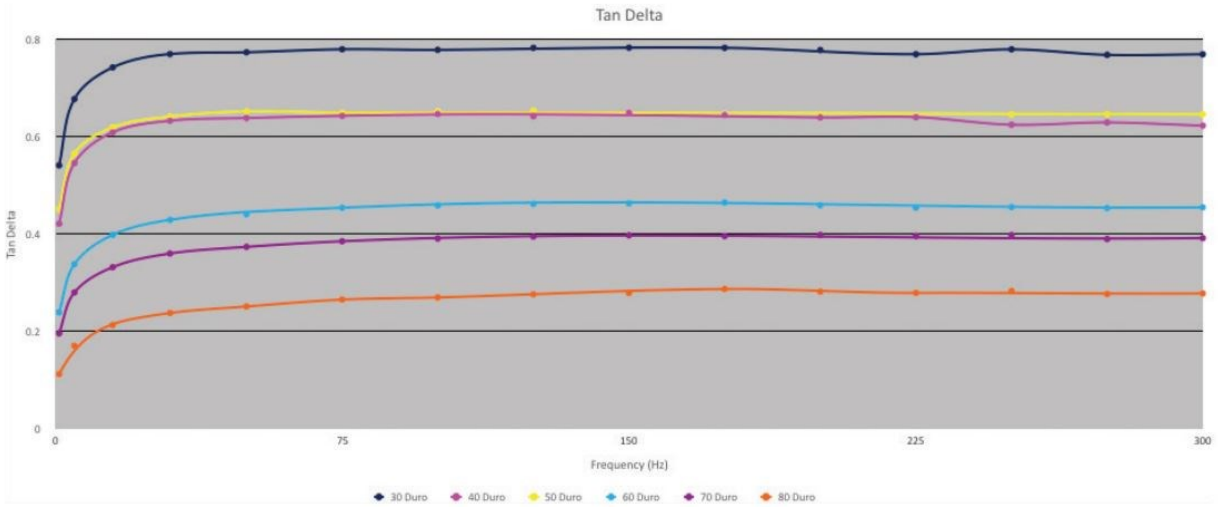

Figure 54: Tan Delta Provided by Sorbothane - Engineering Design Guide

Appendix B – Simulink Model

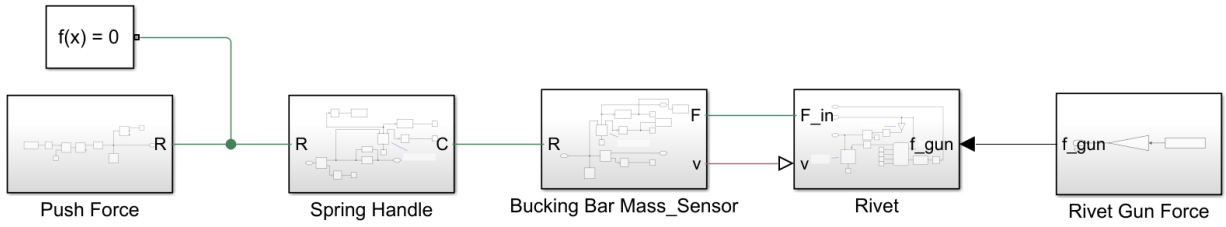

Figure 55: Shows the Simulink model having 5 main blocks.

Figure 56: Rivet gun force block. It loads the generated gun force into the model.

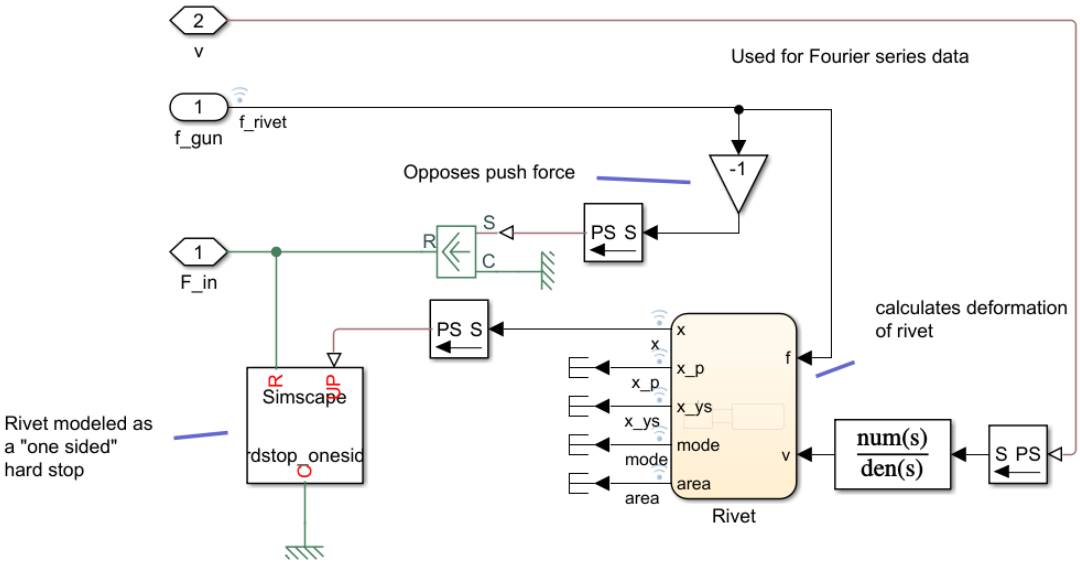

Figure 57: Rivet block that takes the force of the rivet gun as input. It applies the force from the bucking bar on the opposite side.

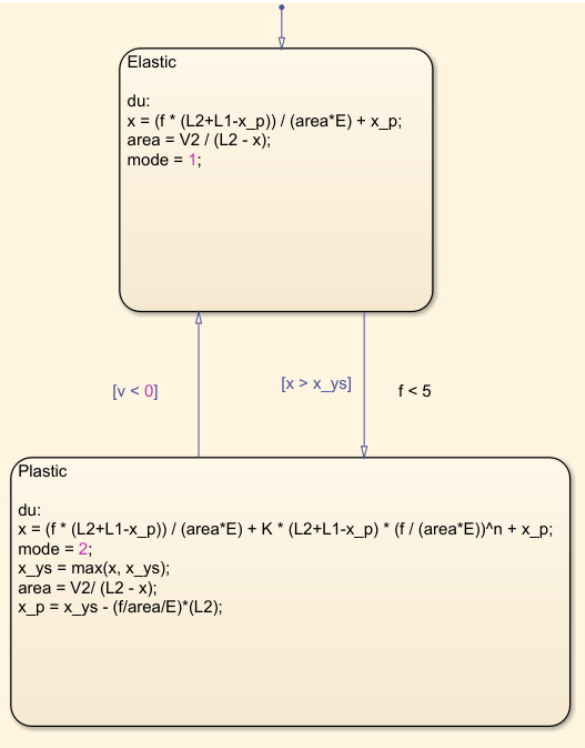

Figure 58: The stress strain curve of the rivet material. It deforms the rivet using the Ramberg-Osgood equation.

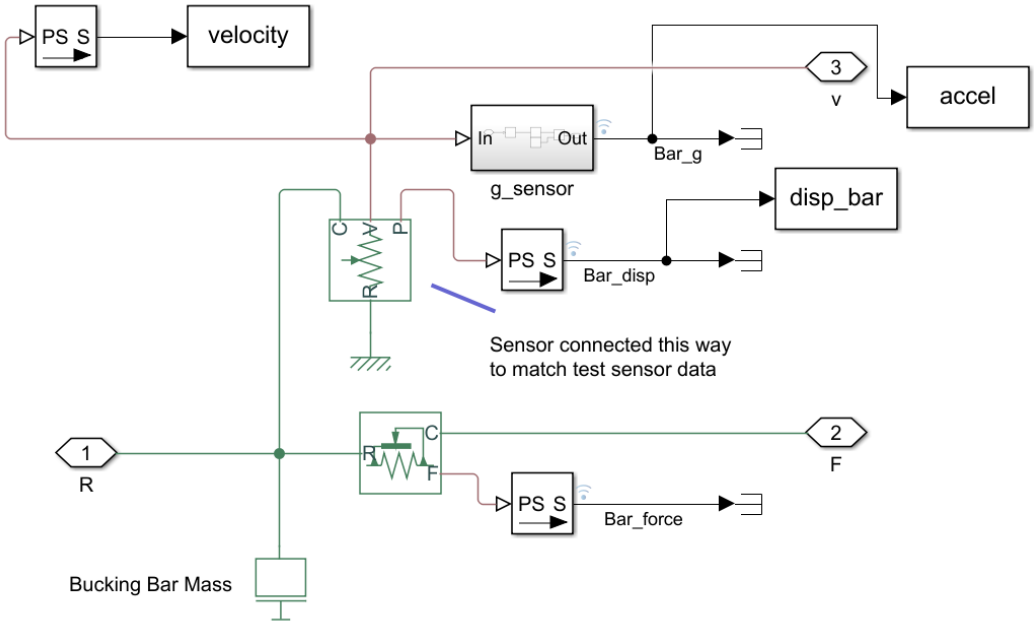

Figure 59: The bucking bar block. It allows the user to set the mass of the bar. It generates its displacement, velocity, and acceleration.

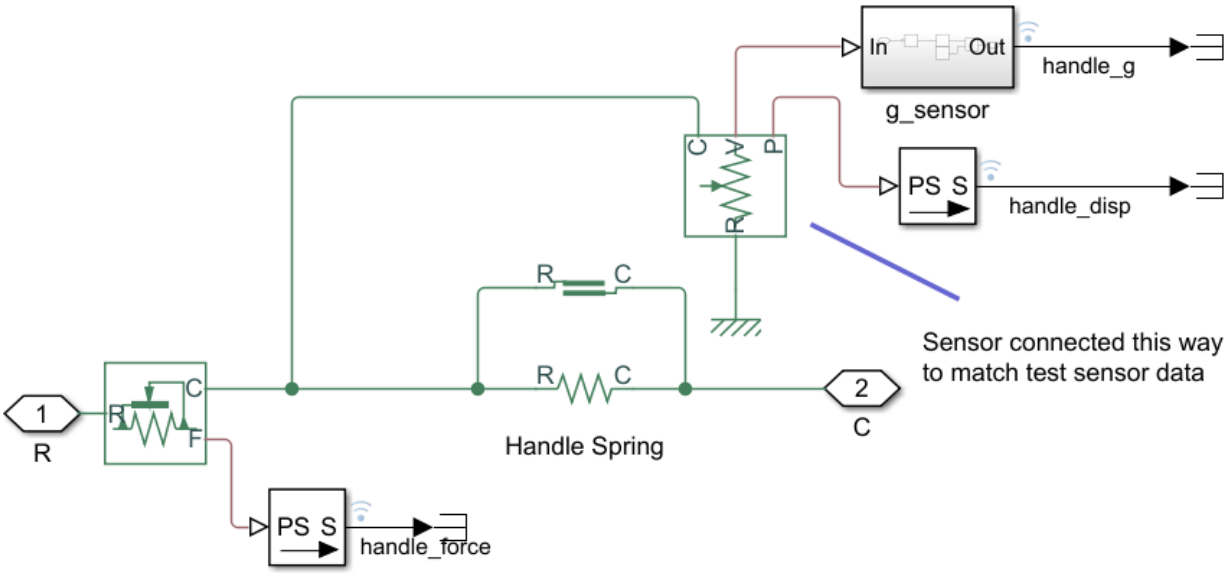

Figure 60: The handle block. It allows the user to set the spring rate, friction, and damping of the system. It generates the displacement, velocity, and acceleration of the handle.

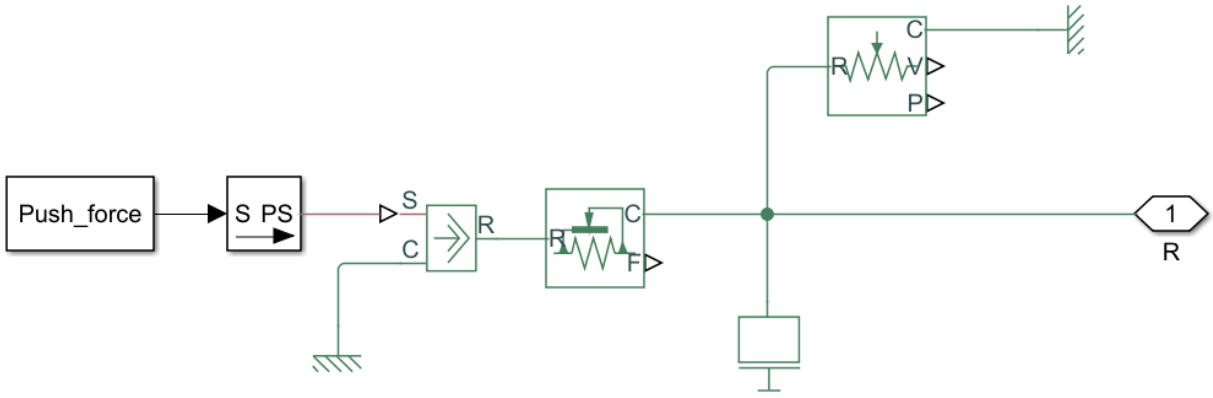

Figure 61: The push force block. It allows the user to choose the push force and set the handle's mass.

Appendix C – Mechanics' Feedback

Subject	Q	Question	P	Y	CA	CS	T
5	1	This tool was easy to use	2	2	2	3	3
5	2	This tool feels comfortable for my hands and wrists while using	2	2	3	1	5
5	3	This tool feels comfortable for my arms and shoulders while using	3	4	2	3	3
5	4	It was easy to make errors using this tools	4	4	5	3	3
5	5	I liked the weight of this tools	3	2	2	2	3
5	6	I can quickly complete tasks using this tools	3	3	3	4	3
5	7	I like the overall feel of this tool when working	3	4	3	3	4
5	8	There was less vibration when using this tool	5	4	3	5	4
5	9	It took a long time to adjust to using this tool	6	5	5	3	3
5	10	I like the handle of this tool	2	4	3	6	4
6	1	This tool was easy to use	4	6	6	4	6
6	2	This tool feels comfortable for my hands and wrists while using	2	6	6	3	3
6	3	This tool feels comfortable for my arms and shoulders while using	3	5	5	3	4
6	4	It was easy to make errors using this tools	4	2	2	3	2
6	5	I liked the weight of this tools	5	4	5	2	4
6	6	I can quickly complete tasks using this tools	5	5	6	4	4
6	7	I like the overall feel of this tool when working	4	5	6	3	5
6	8	There was less vibration when using this tool	1	7	6	5	6
6	9	It took a long time to adjust to using this tool	1	2	2	3	2
6	10	I like the handle of this tool	2	5	4	2	2

Figure 62: Survey questions with the scores provided by the mechanics.

Subject	Question	P	Y	CA	CS	T
5	Now that you have tried this TOOL, what are your initial thoughts about it? Likes/dislikes? What would you change about this TOOL?	This is a production type tool. Know it very well	It worked. Spring? Soft	Spring was just about right. Test mounts hampered the full tool	Spring travel "recole"	Not in love with it. Handle spring is closer
6	Now that you have tried this TOOL, what are your initial thoughts about it? Likes/dislikes? What would you change about this TOOL?	More control is needed at the face of this bar causing more fatigue	This feel like the right tool for this specific application	Love it, dome the handle	Front heavy, spring and handle wave very nice	Handle needs to be domed
5	Any comments on the overall feel of the TOOL?	All good	Better grip but not all good	It worked well	Did not fit my hand, not all tool some test	Fitting of end was wokable, not there yet
6	Any comments on the overall feel of the TOOL?	Good weigth	Smooth	Very smooth, good spring	heavy	Smooth operation/ Good spring tension
5	Any comments on the overall size and shape of the TOOL?	All good	Far better than a rock	Good, could use a little tweeking	Not a good gripping from	Not fitting my hand well
6	Any comments on the overall size and shape of the TOOL?	A little short in length	Good shape and length	Good shape and size	Good shape and length	Good shape and length
5	Any comments on the overall weight of the TOOL?	All good	Not a real concern for me	All good	Worked plane, weight not a problem	All good
6	Any comments on the overall weight of the TOOL?	Well balanced	A little front heavy	Front heavy	Heavy	Well balanced
5	Any comments on the handle supplied with the TOOL?	good	Better than CS tool	All good	Same as above	See all above
6	Any comments on the handle supplied with the TOOL?	Too short but good cushion	Good fit to palm of hand	Should be domed	Cushion	Handle shape hurt palm of hand
5	Any other comments on the vibrations you experienced with the TOOL? More? Less? About the same as the TOOL you typically use for this task?	Same. You have bucked a pivot	Still not much change	Tool took the first hit a lot. Better, not such a shock	Has a large jump at start, must real get after it on the drive.	Pretty much same as typically run in production
6	Any other comments on the vibrations you experienced with the TOOL? More? Less? About the same as the TOOL you typically use for this task?	Same as typical tools, much more vibration than with spring	Much much less	Much much less	Much less vibration, a little jump when bucking	Much less

Figure 63: Questions asked about the tool impressions.

Subje	Question	Response	Rank 1	Rank 2	Rank 3	Rank 4	Rank 5
5	Now that you have tried all the TOOLS, would any of these TOOLS replace TOOL you use at work? Why or why not?	Use CA with plastic form *(Combination of CA and P tool)*					
6	Now that you have tried all the TOOLS, would any of these TOOLS replace TOOL you use at work? Why or why not?	Absolutely. CA and Y proved a severe reduction in vibration transfer & fatigue					
5	Now that you have tried all the TOOLS, rank them from most preferred to least preferred overall	-	P	CA	Y	CS	T
6	Now that you have tried all the TOOLS, rank them from most preferred to least preferred overall	-	CA	Y	CS	T	P
5	What did you like about your most preferred model that made you choose it first?	It is what is used in production					
6	What did you like about your most preferred model that made you choose it first?	Comfort. Good size and weigth					
5	What did you not like about the your least preferred model that made you choose it last?	Size, spring. Fit not good					
6	What did you not like about the your least preferred model that made you choose it last?	Most vbration & fatigue to body					

Figure 64: Questions asked at the end of the day after completing the riveting sessions with all the tools.

Appendix D – Transmissibility Calculation

To calculate the transmissibility, the damping of the system should be found. In the results section it is shown that the damping in the system is $c = 30\ \frac{Ns}{m}$. Using equation 4, the damping ratio of the yellow handle and the new handle was found to be $\zeta_Y = 0.13$ and $\zeta_T = 0.12$ respectively. Using *Figure 65* and the frequency ratio, the expected transmissibility for the yellow handle is $T_{Ye} = 0.09$ and for the new handle $T_{Te} = 0.18$.

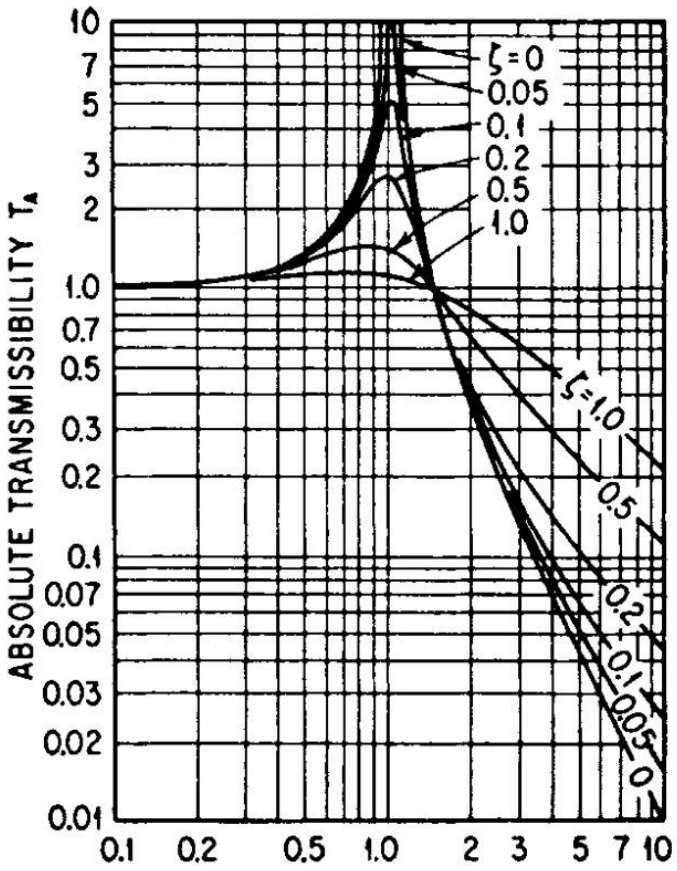

Figure 65: Absolute transmissibility for the rigidly connected, viscous-damped isolation system.

Table 8 and *Table 9* summarize the average peak acceleration values (approximated to the nearest integer) recorded on the bucking bar via the shock accelerometer and on the handle recorded via the triaxial accelerometer.

Table 8: Summarizing the average peak acceleration recorded on the yellow handle during each run on the test bench. The average transmissibility is found to be 0.1044.

Run on test bench	Acceleration on the bar [g]	Acceleration on the handle [g]	Ratio
1	1044	166	0.1585
2	1203	128	0.1063
3	1133	119	0.1055
4	1135	86	0.0758
5	1020	100	0.0983
6	1058	200	0.0949
7	1036	208	0.1033
8	1028	98	0.0955
9	1083	112	0.1038
10	1000	93	0.0932
11	1001	106	0.1059
12	975	112	0.1145

Table 9: Table summarizing the average peak acceleration recorded on the new handle during each run on the test bench. The average transmissibility is found to be 0.0918.

Run on test bench	Acceleration on the bar [g]	Acceleration on the handle [g]	Ratio
1	1039	109	0.1054
2	976	68	0.0694
3	1025	62	0.0608
4	1065	86	0.0812
5	1055	101	0.096
6	967	93	0.0961
7	988	117	0.1182
8	1079	99	0.0918
9	1071	100	0.0933
10	981	98	0.1003
11	996	109	0.1093
12	985	80	0.0807